Chapter 2
Intra-oceanic Subduction Zones

T.V. Gerya

2.1 Introduction

According to the common definition, intra-oceanic subduction brings oceanic slabs under the overriding plates of oceanic origin. As a consequence oceanic magmatic arcs are formed worldwide (Fig. 2.1) with typical examples such as the Izu-Bonin-Mariana arc, the Tonga-Kermadec arc, the Vanuatu arc, the Solomon arc, the New Britain arc, the western part of the Aleutian arc, the South Sandwich arc and the Lesser Antilles arc (Leat and Larter 2003). Intra-oceanic subduction zones comprise around 17,000 km, or nearly 40%, of the subduction margins of the Earth (Leat and Larter 2003). Indeed, intra-oceanic arcs are less well studied than continental arcs since their major parts are often located below sea level, sometimes with only the tops of the largest volcanoes forming islands. Intra-oceanic subduction zones are sites of intense magmatic and seismic activities as well as metamorphic and tectonic processes shaping out arc compositions and structures. During an ocean closure (e.g., Collins 2003) such arcs may collide with continental margins creating distinct structural and compositional record in continental orogens (such as in Himalaya, Burg 2011) which makes them of particular interest for the present book.

Several years ago Leat and Larter (2003) published a comprehensive review on intra-oceanic subduction systems. The review focused on tectonic and magmatic processes in intra-oceanic arcs and was mainly based on observational constraints. In addition, Schellart et al. (2007) compiled detailed nomenclature and taxonomy of Subduction zones worldwide. The following major characteristics of intra-oceanic subduction zones can be summarized (Leat and Larter 2003; Schellart et al. 2007 and references therein)

- *Convergence rates* vary from ca 2 cm/yr in the Lesser Antilles arc to 24 cm/yr in the northern part of the Tonga arc, the highest subduction rates on Earth. Typical rates are in the range 5–13 cm/yr. Intra-arc variations are almost as large as inter-arc ones.
- *Ages of subducting slabs* range from ca 150 Ma (Pacific Plate subducting beneath the Mariana arc) to close to zero age (along part of the Solomon arc). Along-arc variations in slab ages are typically not large ($\pm$10 Ma). There are indeed large variations in the topography of the subducting plates (up to 5 km, Fig. 2.1): some are relatively smooth, some contain ridges and seamounts that affect subduction and arc tectonics.
- *Sediment thicknesses* are notably variable (from 70 m to >6 km, typically 150–650 m). Sediment cover is commonly thinner over basement highs. Variations in thickness and composition of subducted sediments are probably greatest where arcs are close to, or cut across, ocean–continent boundaries.
- *Accretion v. non-accretion.* Most modern intra-oceanic arcs are non-accreting, i.e. there is little or no net accumulation of off-scrapped sediment forming accretionary complexes. In other words, all the sediments arriving at the trenches are subducted (over a period) into the mantle. The two exceptions are the Lesser Antilles and Aleutian arcs, both of which have relatively high sediment inputs and where accretionary complexes have formed.

T.V. Gerya
Geophysical Fluid Dynamics Group, Department of Earth Sciences, Institute of Geophysics, Swiss Federal Institute of Technology (ETH-Zurich), Sonneggstrasse, 5, 8092 Zurich, Switzerland
e-mail: taras.gerya@erdw.ethz.ch

D. Brown and P.D. Ryan, *Arc-Continent Collision*, Frontiers in Earth Sciences,
DOI 10.1007/978-3-540-88558-0_2,

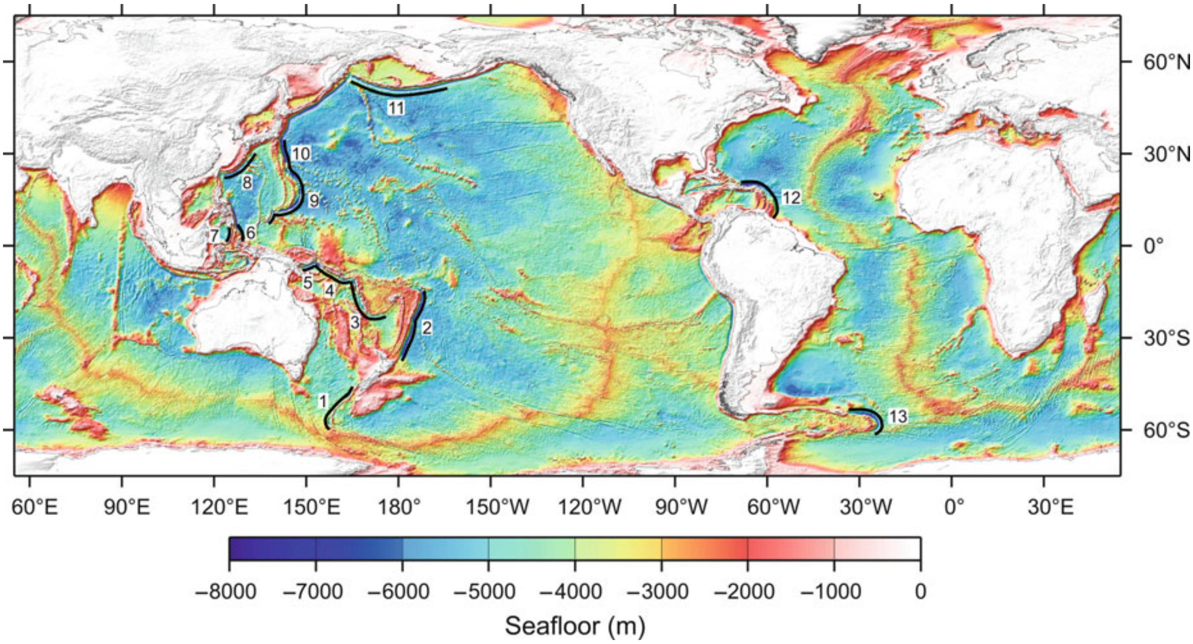

Fig. 2.1 Location of modern intra-oceanic subduction zones. The trenches of these subduction systems are indicated by heavy black lines, and identified by numbers that correspond to those of Leat and Larter (2003): 1 – MacQuarie; 2 – Tonga-Kermadec; 3 – Vanuatu (New Hebrides); 4 – Solomon; 5 – New Britain; 6 – Halmahara; 7 – Sangihe; 8 – Ryuku; 9 – Mariana; 10 – Izu-Bonin (Ogasawara); 11 – Aleutian; 12 – Lesser Antilles; 13 – South Sandwich.

- *Back-arc extension.* Most of the arcs have closely associated back-arc rifts. Only the Solomon and Aleutian arcs are exceptions in having no apparent back-arc extension. In most cases, the back-arc extension takes the form of well-organized seafloor spreading for at least part of the length of the back-arc. Such spreading appears to follow arc extension and rifting in at least some cases.
- *Arc thicknesses* depend on arc maturity, tectonic extension or shortening, and the thickness of pre-arc basement. Only approximately, therefore, is it true to say that the thin crusts (e.g. of the South Sandwich and Izu-Osgaswara) arcs represent arcs in the relatively early stages of development, whereas arcs with thicker crusts are more mature (e.g. the Lesser Antilles and Aleutian arcs).
- *Pre-arc basements* of the arcs are very variable. Only one intra-oceanic arc (the Aleutian arc) is built on normal ocean crust. The others are built on basements comprising a range of oceanic lithologies, including ocean crust formed at back-arc spreading centres, earlier intra-oceanic arcs, accretionary complexes and oceanic plateaux. This also points out toward complexity of intraoceanic subduction (re)initiation scenarios.

In the recent years significant new literature on intra-oceanic subduction appeared (in particular, on high-resolution seismic studies of arc structures and on numerical modeling of intra-oceanic subduction) that should be added to the state-of-the-art knowledge which is one of the reasons for writing this chapter. Also, taking into account that the present volume mainly concentrates on arc collision processes I will focus the review on relatively shallow portions of intraoceanic subduction-arc system from which the record can be preserved in the resulting collision zones (e.g. Burg 2011). The following major issues will be discussed in the review

- Initiation of intra-oceanic subduction
- Internal structure and composition of arcs
- Subduction channel processes
- Dynamics of crustal growth
- Geochemistry of intra-oceanic arcs

In order to keep a cross-disciplinary spirit of modern intra-oceanic subduction studies often combining observational constrains with results of numerical geodynamic modelling the later will be used here for visualizing various subduction-related processes instead of more traditional hand-drawn cartoons.

2.2 Initiation of Intra-oceanic Subduction

It is yet not entirely clear how subduction in general and intraoceanic subduction in particular is initiated. The gravitational instability of an old oceanic plate is believed to be the main reason for subduction (Vlaar and Wortel 1976; Davies 1999). Oceanic lithosphere becomes denser than the underlying asthenosphere within 10–50 Ma after it forms in a mid-ocean ridge due to the cooling from the surface (Oxburg and Parmentier 1977; Cloos 1993; Afonso et al. 2007, 2008). However, despite the favourable gravitational instability and ridge-push, the bending and shear resistance of the lithosphere prevent subduction from arising spontaneously (McKenzie 1977). Consequently, the following question arises: what forces can trigger subduction (besides the negative buoyancy and ridge-push)? At least 12 hypotheses have been proposed to answer this question:

1. Plate rupture within an oceanic plate or at a passive margin (e.g. McKenzie 1977; Dickinson and Seely 1979; Mitchell 1984; Müeller and Phillips 1991).
2. Reversal of the polarity of an existing subduction zone (e.g. Mitchell 1984).
3. Change of transform faults into trenches (e.g. Uyeda and Ben-Avraham 1972; Hilde et al. 1976; Karson and Dewey 1978; Casey and Dewey 1984).
4. Sediment or other topographic loading at continental/arc margins (e.g. Dewey 1969; Fyfe and Leonardos 1977; Karig 1982; Cloetingh et al. 1982; Erickson 1993; Pascal and Cloetingh 2009).
5. Forced convergence at oceanic fracture zones (e.g. Müeller and Phillips 1991; Toth and Gurnis 1998; Doin and Henry 2001; Hall et al. 2003; Gurnis et al. 2004).
6. Spontaneous initiation of retreating subduction (Fig. 2.2) due to a lateral thermal buoyancy contrast at oceanic fracture zones separating oceanic plates of contrasting ages (e.g. Gerya et al. 2008; Nikolaeva et al. 2008; Zhu et al. 2009).
7. Tensile decoupling of the continental and oceanic lithosphere due to rifting (Kemp and Stevenson 1996).
8. Rayleigh-Taylor instability due to a lateral compositional buoyancy contrast within the lithosphere (Niu et al. 2003).
9. Addition of water into the lithosphere (Regenauer-Lieb et al. 2001; Van der Lee et al. 2008).
10. Spontaneous thrusting (Fig. 2.3) of the buoyant continental/arc crust over the oceanic plate (Mart et al. 2005; Nikolaeva et al. 2010; Goren et al. 2008).
11. Small-scale convection in the sub-lithospheric mantle (Solomatov 2004).
12. Interaction of thermal-chemical plumes with the lithosphere (Ueda et al. 2008).

In the recent review by Stern (2004 and references therein) two major types of subduction initiation scenarios applicable to intraoceanic subduction are proposed based on both theoretical considerations and natural data: induced and spontaneous. Induced subduction nucleation may follow continuation of plate convergence after jamming of a previously active subduction zone (e.g. due to arrival of a buoyant crust to the trench). This produces regional compression, uplift and underthrusting that may yield a new subduction zone in a different place. Two subtypes of induced initiation, transference and polarity reversal, are distinguished (Stern 2004 and references therein). Transference initiation moves the new subduction zone outboard of the failed one. The Mussau Trench and the continuing development of a plate boundary SW of India in response to Indo–Asian collision are the best Cenozoic examples of transference initiation processes (Stern 2004 and references therein). Polarity reversal initiation also follows collision, but continued convergence in this case results in a new subduction zone forming behind the magmatic arc; the response of the Solomon convergent margin following collision with the Ontong Java Plateau (Stern 2004 and references therein) and dramatic reorganization of the tectonic plate boundary in the New Hebrides region (Pysklywec et al. 2003 and references therein) are suggested to be the examples of this mode.

Spontaneous nucleation results from inherent gravitational instability of sufficiently old oceanic lithosphere

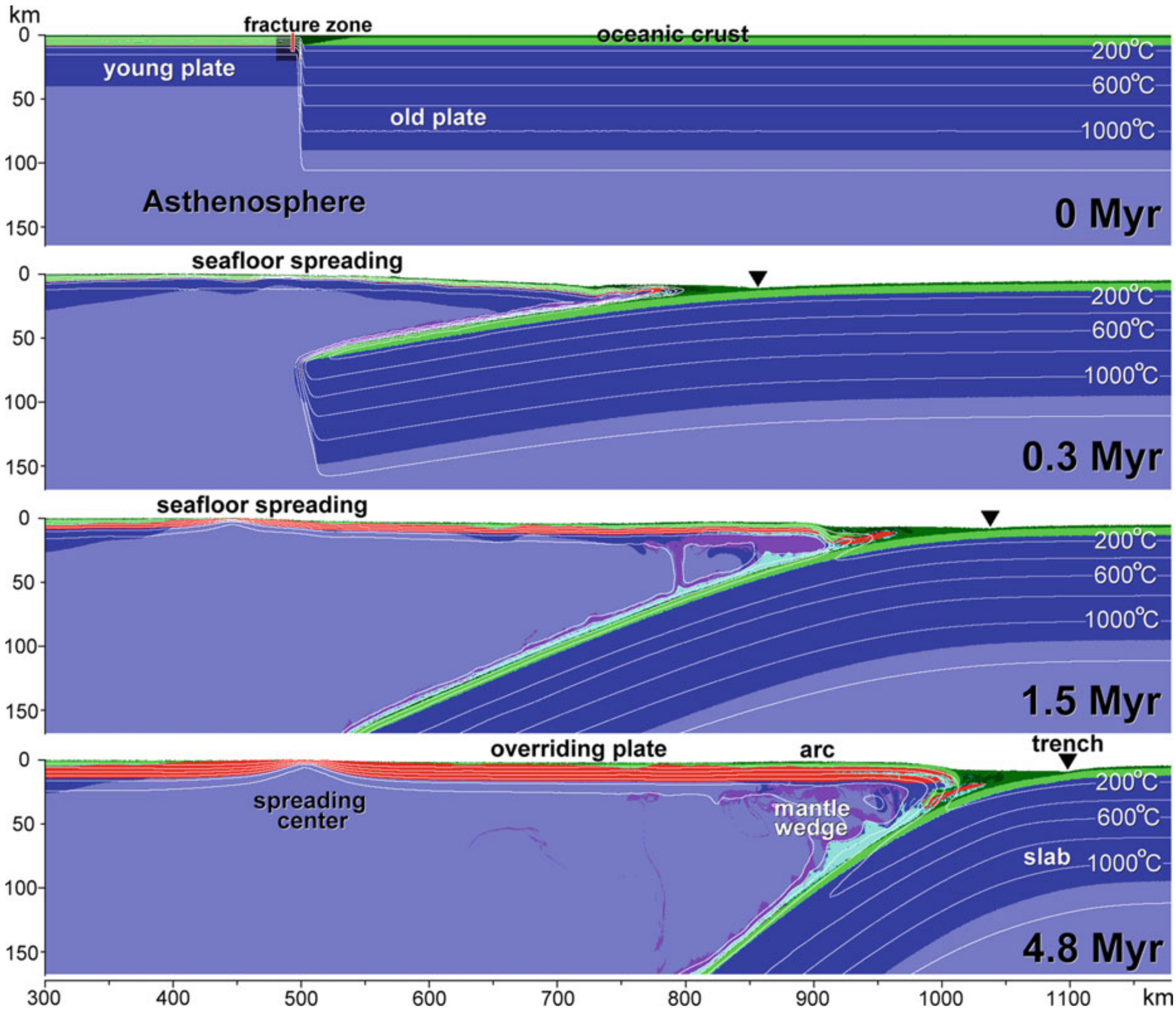

Fig. 2.2 Dynamics of spontaneous initiation of retreating subduction at a transform/fracture zone separating oceanic plates of contrasting ages. Results from 2D numerical experiments by Gerya et al. (2008).

compared to the underlying mantle, which is also the main reason for operating of the modern regime of plate tectonics. It is widely accepted (e.g. Stern 2004 and references therein) that intra-oceanic subduction can initiate spontaneously either at a transform/fracture zone (Fig. 2.2) or at a passive continental/arc margin (Fig. 2.3), in a fashion similar to lithospheric delamination. According to the theoretical prediction (e.g. Stern 2004) and numerical modeling results (e.g. Gerya et al. 2008; Nikolaeva et al. 2008; Zhu et al. 2009) spontaneous initiation across a fracture zone separating oceanic plates of contrasting ages associates with an intense seafloor spreading (Fig. 2.2, 0.3–1.5 Myr), as asthenosphere wells up to replace sunken lithosphere of the older plate. This is the presumable origin of most boninites and ophiolites (Stern 2004 and references therein). Such initiation process assumed to have produced new subduction zones along the western edge of the Pacific plate during the Eocene (Stern 2004 and references therein). Development of self-sustaining one-sided subduction is marked by the beginning of down-dip slab motion, formation of the mantle wedge and appearance of the magmatic arc at 100–200 km distance from the retreating trench (Fig. 2.2).

Passive continental/arc margin collapse (Fig. 2.3) is driven by the geometry of the margin, where relatively thick (20–35 km) low-density continental/arc crust is

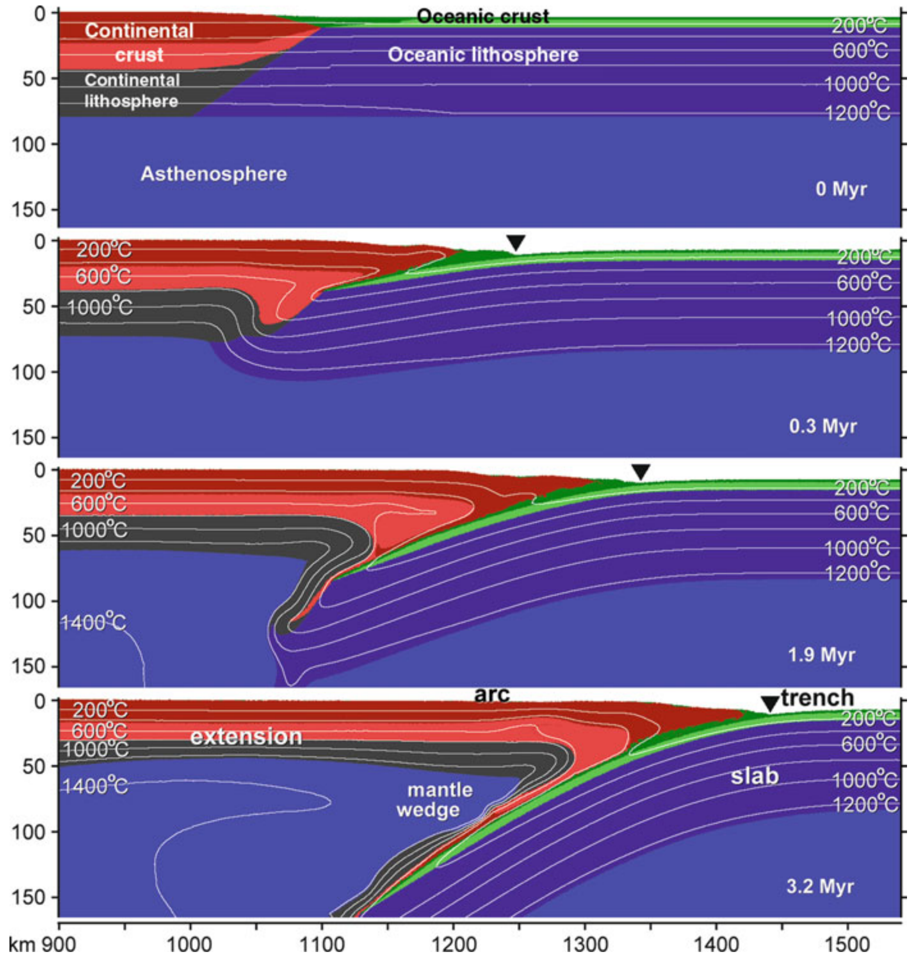

Fig. 2.3 Dynamics of spontaneous subduction initiation at a passive continental/arc margin. Results from 2D numerical experiments by Nikolaeva et al. (2010).

bounded laterally by significantly more dense oceanic lithosphere. When during the margin evolution forces generated from this lateral density contrast become big enough to overcome the continental/arc crust strength then this crust starts to creep over the oceanic one (Fig. 2.3, 0.3 Myr). This causes deflection of the oceanic lithosphere (Fig. 2.3, 0.3 Myr) and may actually lead to its delamination from the continental/arc lithosphere (Fig. 2.3, 0.3–1.9 Myr) thus triggering retreating subduction process (Fig. 2.3, 1.9–3.2 Myr). This type of subduction nucleation has been successfully modelled with both analogue (Mart et al. 2005; Goren et al. 2008) and numerical (Nikolaeva et al. 2010) techniques. No undeniable modern example of such ongoing subduction initiation is yet known: a possible recent exception is suggestion for subduction/overthrusting initiation at the eastern Brasilian margin (Marques et al. 2008). Indeed, Goren et al. (2008) speculated that such type of initiation was relevant in the past for two active intra-oceanic subduction systems in which Atlantic lithosphere is being subducted: the Lesser-Antilles and the South Sandwich subduction systems. Also, Masson et al. (1994) and Alvarez-Marron et al. (1996, 1997) argued that an arrested subduction zone nucleation can be distinguished in the North Iberian Margin based on structural and seismic data.

Both spontaneous and induced subduction initiation can be potentially distinguished by the record left on the upper plates: induced nucleation begins with strong compression and uplift, whereas spontaneous one begins with rifting and seafloor spreading (Stern 2004).

2.3 Internal Structure of Intra-oceanic Arcs

Internal structure and compositions of intra-oceanic arcs are strongly variable depending on both the pre-existing plate structure and on the dynamics of subduction and associated crustal growth (e.g. Leat and Larter 2003). In addition, deep parts of the arcs are mainly reconstructed based on seismic data and fragmentary records left in orogens after arc-continent collisions, which creates further uncertainties for interpretations of intra-oceanic arc structures. As was indicated by Tatsumi and Stern (2006) understanding how continental crust forms at intra-oceanic arcs requires knowledge of how intra-oceanic arcs form and mature with key questions being:

1. What is the nature of the crust and mantle in the region prior to the beginning of subduction?
2. How does subduction initiate and initial arc crust form?
3. How do the middle and lower arc crusts evolve?
4. What are the spatial changes of arc magma and crust compositions of the entire arc?

In this respect, in addition to robust natural data, realistic self-consistent numerical modelling of subduction and associated crustal growth (e.g., Nikolaeva et al. 2008; Kimura et al. 2009; Sizova et al. 2009; Gerya and Meilick 2011) can complement the interpretations of details and variability in arc structures. Figure 2.4 shows a schematic cross-section across a mature intra-oceanic arc corresponding to the retreating subduction regime. The cross-section is based on recent results of numerical petrological-thermomechanical modelling (Gerya and Meilick 2011). The following major structural components of the arc can be distinguished based on this scheme and natural data: (a) accretion prism (if present), (b) pre-arc basement (c) serpentinized fore-arc including subduction channel composed of tectonic melange, (d) magmatic crust, (e) sub-arc lithosphere (cumulates?, replacive rocks?, intercalation of crustal and mantle rocks and melts?), (f) back-arc region with new oceanic floor and a spreading center and (g) paleo-arc (in the rear part

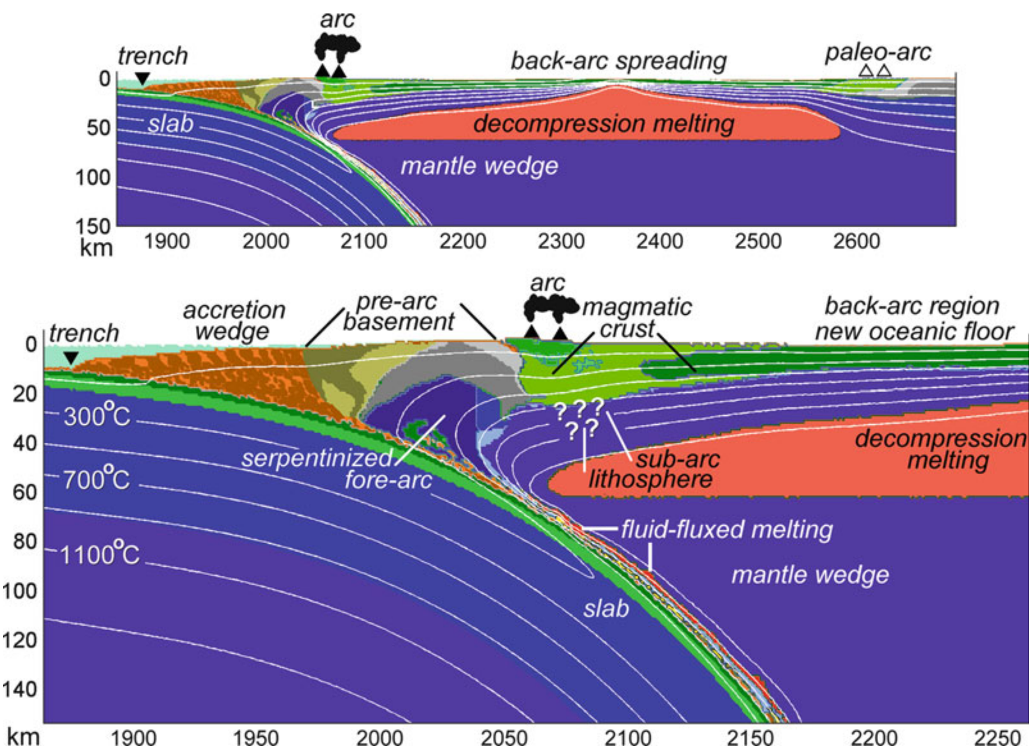

Fig. 2.4 Schematic cross-section of an intra-oceanic arc associated with retreating subduction. Results from 2D numerical experiments by Gerya and Meilick (2011).

of the back-arc spreading domain). Obviously this structure is non-unique and significant variations can be expected in both nature (e.g. Tatsumi and Stern 2006; Takahashi et al. 2007, 2009; Kodaira et al. 2006, 2007, 2008) and models (e.g. Nikolaeva et al. 2008; Sizova et al. 2009; Gerya and Meilick 2011), depending on arc history, subduction dynamics and sub-arc variations in melt production intensity, distribution and evolution (e.g. Tamura 1994; Tamura et al. 2002; Honda et al. 2007; Zhu et al. 2009).

Recently new high-resolution data (see Calvert 2011) were obtained concerning seismic structure of the arc crust in Izu-Bonin-Mariana system (e.g. Takahashi et al. 2007, 2009; Kodaira et al. 2006, 2007, 2008). These data suggest that lateral variations in crustal thickness, structure and composition occur both along and across intra-oceanic arcs (e.g. Figs. 4.1–4.7 in Calvert 2011; Kodaira et al. 2006; Takahashi et al. 2009). Such variations are interpreted as being the results of laterally and temporally variable magmatic addition and multiple episodes of fore-arc, intra-arc and back-arc extension (e.g. Takahashi et al. 2007, 2009; Kodaira et al. 2006, 2007, 2008). Seismic models demonstrate notable velocity variations (Fig. 4.1 in Calvert 2011) within the arc middle and lower crusts, which are interpreted to be respectively of intermediate to felsic and mafic compositions (e.g. Takahashi et al. 2007). In the regions of the maximal thickness (around 20 km, Fig. 4.1 in Calvert 2011) the oceanic-island-arc crust is composed of a volcanic-sedimentary upper crust with velocity of less than 6 km/s, a middle crust with velocity of ~6 km/s, laterally heterogeneous lower crust with velocities of ~7 km/s, and unusually low mantle velocities (Takahashi et al. 2009; also see crust–mantle transition layer in Fig. 4.1a, b in Calvert 2011). Petrologic modeling of Takahashi et al. (2007) suggests that the volume of the lower crust, presumably composed of restites and olivine cumulates remained after the extraction of the middle crust, should be significantly larger than is observed on the seismic cross-sections. Therefore, such mafic-ultramafic part of the lower crust (if at all present in the arcs, e.g. Jagoutz et al. 2006) should have seismic properties similar to the mantle ones and consequently look seismically as a part of the mantle lithosphere.

There are notable uncertainties in interpreting seismic structures of intra-oceanic arcs, which are related to current uncertainties in understanding melt differentiation processes under the arcs. As summarised by Leat and Larter (2003) the major element composition of magmas feeding arcs from the mantle has been and remain (e.g. Jagoutz et al. 2006) a subject of debate, particularly regarding the Mg and A1 contents of primary magmas. Mafic compositions in arcs have variable MgO content, but with a clear cut-off at about 8 wt% MgO or even less (in the case of mature arcs). High-MgO, primitive non-cumulate magmas have indeed been identified in many arcs, but they are always volumetrically very minor (Davidson 1996). One question is, therefore, whether the MgO cut-off point represents composition of the mantle-derived parental magmas, or whether the mantle-derived parental magmas are significantly more MgO-rich (>10% MgO), but are normally unable to reach the surface and erupt. It has been argued that they have difficulty in traversing the crust without encountering magma chambers because of their relatively high density (Smith et al. 1997; Leat et al. 2002). In addition, as argued by Pichavant and Macdonald (2003) only the most water-poor primitive magmas are able to traverse the crust without adiabatically freezing.

It should, however, be mentioned that the above explanations are not fully satisfactory in explaining the “MgO-paradox”. First, as has recently been demonstrated numerically (Gerya and Burg 2007; Burg et al. 2009) local density contrast between rising dense magmas and surrounding crustal rocks plays only a secondary role compared the rheology of the crust. According to the numerical results, in case of relatively strong lower crust even very dense ultramafic magmas can easily reach the surface given that they are generated below a sufficiently dense and thick mantle lithosphere. Second, when differentiation of the parental high-MgO mantle-derived magma takes place inside the arc crust, significant volumes of high-MgO cumulates should be produced. Fractionation models indicate that 15–35% crystallization is necessary to lower the MgO content adequately (e.g., Conrad and Kay 1984). Such cumulates should either (1) form a major component below the seismic Moho (e.g. Kay and Kay 1985; Müntener et al. 2001; Takahashi et al. 2007) or (2) delaminate and sink back into the mantle (e.g., Kay and Kay 1991, 1993; Jull and Kelemen 2001). The delamination theory is presently favoured based on the lack of appropriate upper mantle rocks brought to the surface in continental regions (e.g. Rudnick and Gao 2003), the absence of primitive cumulate rocks in the exposed Talkeetna paleo-island arc crust section (Kelemen et al. 2003) and evidence for active foundering of the lower continental crust below the southern Sierra Nevada, California (Zandt et al. 2004; Boyd et al. 2004).

An alternative explanation of magma differentiation processes in the arcs has recently been proposed by Jagoutz et al. (2006) based on geochemical data from the Kohistan paleo-arc in NW Pakistan. According to this hypothesis the melt rising through the Moho boundary of an arc has already a low-MgO basaltic–andesitic composition, while the primary magma generated in the mantle wedge is a high-MgO primitive basaltic liquid. Fractionation of the mantle-derived melt takes place in the mantle lithosphere within km-scaled isolated conduits (replacive channels). The dunitic ultramafic bodies found in the lowermost section of the Kohistan paleo-arc are interpreted as remnants of such melt channels through which the low-MgO (i.e. differentiated) lower-crustal intrusive mafic sequence was fed. As suggested by Jagoutz et al. (2007) such differentiation within the upper mantle is an important lower crust-forming process which can also explain the absence of high-MgO cumulates in the lower crust of exposed island arcs (e.g., Kelemen et al. 2003).

2.4 Subduction Channel Processes

Subduction channel development is an important component of intra-oceanic arc evolution (Fig. 2.4). Processes taking place in the subduction channel lives notable and directly accessible record at the surface in form of exhumed high- and ultrahigh-pressure rocks complexes (e.g., Ernst 1977; Cloos 1982; Shreve and Cloos 1986; Hermann et al. 2000; Abbott et al. 2006; Federico et al. 2007; Krebs et al. 2008). Subduction channel processes may also contribute to a magmatic record through deep subduction and melting of hydrated rock mélanges formed in the channel (e.g., Gerya and Yuen 2003; Gerya et al. 2006; Castro and Gerya 2008; Zhu et al. 2009).

It is widely accepted that the deep burial of high pressure metamorphic rocks in intra-oceanic settings is due to subduction of these rocks with the downgoing slab. However, the mechanisms of their exhumation remain subject of discussion and several models have been proposed (e.g., Cloos 1982; Platt 1993; Maruyama et al. 1996; Ring et al. 1999). According to the most popular corner flow model (Hsu 1971; Cloos 1982; Cloos and Shreve 1988a, b; Shreve and Cloos 1986; Gerya et al. 2002), exhumation of high-pressure metamorphic crustal slices at rates on the order of the plate velocity is driven by forced flow in a wedge-shaped subduction channel.

Gerya et al. (2002) investigated numerically the self-organizing evolution of the accretionary wedge and the subduction channel during intra-oceanic subduction (Fig. 2.5). In this model the geometry of the accretionary wedge and the subduction channel are neither prescribed nor assumed to represent a steady state. Instead, the system is free to evolve, starting from an imposed early stage of subduction, being controlled by the progressive modification of the thermal, petrological, and rheological structure of the subduction zone. In this evolution, upward migration of the aqueous fluid released from the subducting slab and progressive hydration of the mantle wedge play a dominant role. The following conclusions have been made based on numerical results (Gerya et al. 2002):

- Burial and exhumation of high-pressure metamorphic rocks in subduction zones are likely affected by progressive hydration (serpentinization) of the fore-arc mantle lithosphere (e.g. Schmidt and Poli 1998). This process controls the shape and internal circulation pattern of a subduction channel. Widening of the subduction channel due to hydration of the hanging wall mantle results in the onset of forced return flow in the channel. This may explain why the association of high- and/or ultrahigh-pressure metamorphic rocks with more or less hydrated (serpentinized) mantle material is often characteristic for high-pressure metamorphic complexes. Complicated non-steady geometry of weak hydrated subduction channels (Figs. 2.7, 2.9 and 2.11) was also predicted numerically (Gerya et al. 2006; Gorczyk et al. 2006, 2007a; Nikolaeva et al. 2008). This geometry forms in response to non-uniform water release from the slab that is controlled by metamorphic (dehydration) reactions in subducting rocks. Depleted mantle rocks from the base of the arc lithosphere and newly formed magmatic arc crust can be included into the channels

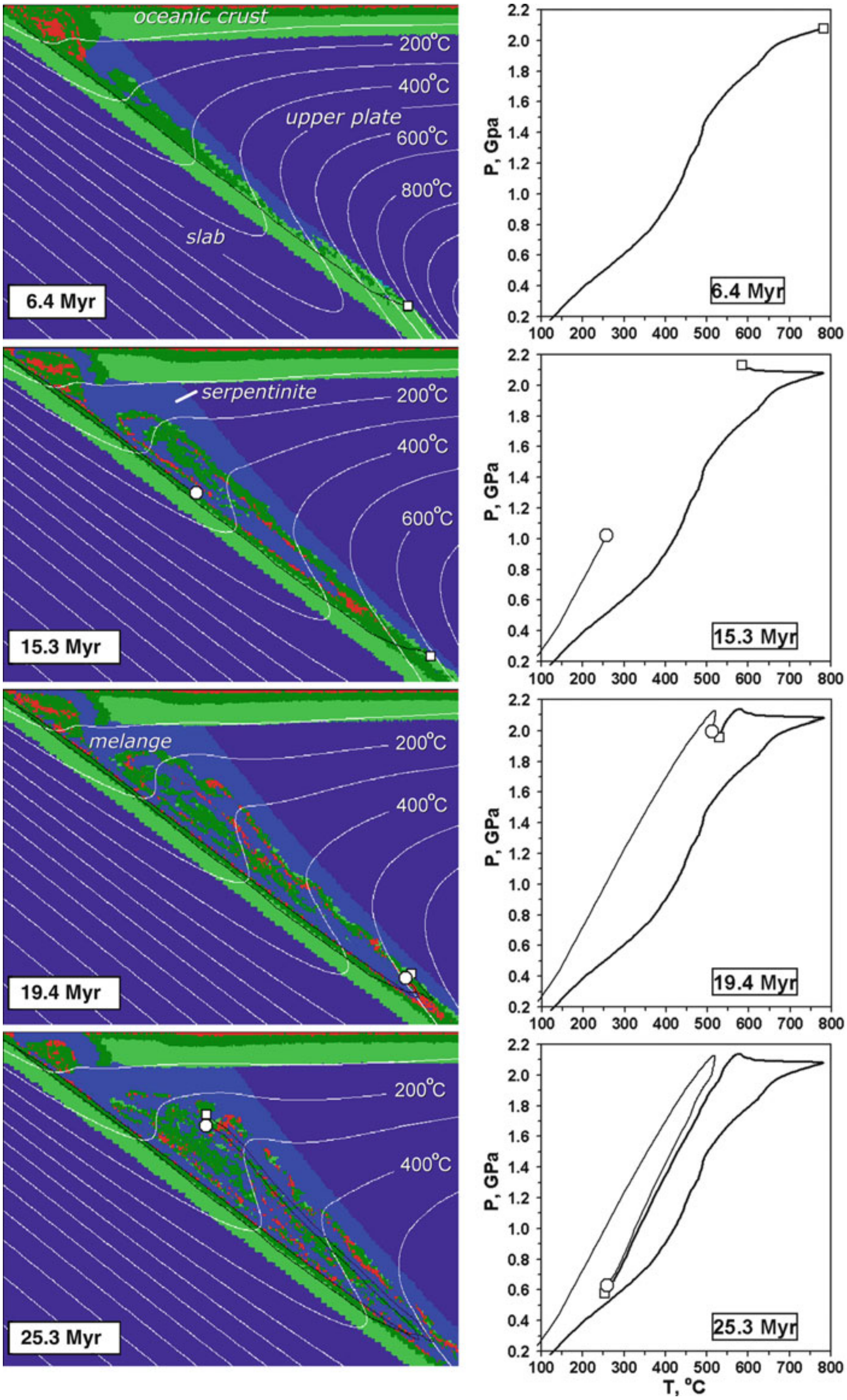

Fig. 2.5 Spontaneous development of weak serpentinized subduction channel during intra-oceanic subduction. Left column – development of the lithological field and isotherms (*white lines*, °C). Right column – development of P–T paths for two rock fragments (see *open circle* and *open rectangle* in the left column). Results from 2D numerical modelling by Gerya et al. (2002).

(Figs. 2.11 and 2.12) at a mature stage of subduction (Nikolaeva et al. 2008).

- The shape of the P–T path, and the maximum P–T conditions achieved by an individual high-pressure metamorphic rock, depend on the specific trajectory of circulation in the subduction channel (Fig. 2.5). Both clockwise and counterclockwise P–T paths are possible for fragments of oceanic crust that became involved in the circulation. Counterclockwise P–T paths are found for slices that are accreted to the hanging wall at an early stage of subduction, and set free by the progress of hydration and softening in a more evolved stage, returning towards the surface in a cooler environment. On the other hand, slices that were involved in continuous circulation, or that entered the subduction zone when a more stable thermal structure was already achieved, reveal exclusively clockwise trajectories. Model also indicates that P–T trajectories for the exhumation of high-pressure rocks in subduction channel fall into a P–T field of stability of antigorite in the mantle wedge (Fig. 2.6c).
- An array of diverse, though interrelated, P–T paths (Fig. 2.6c) rather than a single P–T trajectory is expected to be characteristic for subduction-related metamorphic complexes. The characteristic size and shape of the units with an individual history depend on the effective viscosity of the material in the subduction channel. Lower viscosities result in smaller characteristic length scales for coherent units and a marked contrasts between adjacent slices, a structure commonly termed melange, while higher viscosities favour the formation of extensive coherent nappe-like slices.

These conclusions based on relatively simple low-viscosity serpentinized subduction channel model (Figs. 2.5 and 2.6a) were recently supported by petrological studies (e.g. Federico et al. 2007; Krebs et al. 2008) of subduction-related serpentinite mélanges. For example, Federico et al. (2007) tested the serpentinized channel hypothesis by investigating a serpentinite mélange in the Western Alps, which contains exotic mafic and metasedimentary tectonic blocks, recording heterogeneous metamorphic evolutions and variable high-pressure ages. The peak metamorphic conditions range from eclogite- to garnet-blueschist-facies. The structural evidence and the pressure–temperature paths of the different blocks suggest coupling between blocks and matrix, at least in the blueschist facies. ^{39}Ar-^{40}Ar dating indicates eclogite-facies peak at ca. 43 Ma and blueschist-facies peak at ca. 43 and 40 Ma in different blocks, respectively. These data point to diachronous metamorphic paths resulting from independent tectonic evolutions of the different slices (compare with Figs. 2.5 and 2.6).

Krebs et al. (2008) presented coupled petrological and geochronological evidence from serpentinite melanges of the Rio San Juan Complex, Dominican Republic (Hispaniola) formed by intra-oceanic Caribbean subduction. It has been demonstrated that dispersed blocks of various types of metamorphic rocks in the mélanges provide fossil evidence for the dynamics of the subduction zone channel between 120 and 55 Ma. Based on three exemplary samples of eclogite and blueschist, a series of different but interrelated P–T–time paths was delineated. Eclogites indicate a low P/T gradient during subduction and record conditions in the nascent stages of the subduction zone with an anticlockwise P–T path (compare with Fig. 2.5, 6.4–15.3 Myr). Other blocks record the continuous cooling of the evolving subduction zone and show typical clockwise P–T-paths (compare with Fig. 2.5, 15.3–25.3 Myr). Omphacite blueschists correspond to the mature subduction zone recording very high ("cold") P/T gradients. Cooling rates and exhumation rates of the metamorphic blocks were estimated to be 9–20°C/Ma and 5–6 mm/a, respectively. The derived P–T–time array is compared with the serpentinized channel models (Gerya et al. 2002) with convergence rates of 10–40 mm/a resulting in an increasingly more funnel-shaped subduction channel system with time (Fig. 2.5). The numerically derived array of simulated P–T–time paths as well as the calculated rates of exhumation and cooling agree well with the P–T–time data derived from the metamorphic blocks of the Rio San Juan serpentinite mélanges when convergence rates of 15–25 mm/a are chosen (Krebs et al. 2008). This value is also in accord with available paleogeographic reconstructions calling for a long-term average of 22 mm/a of orthogonal convergence. On the basis of the comparison, the onset of subduction in the Rio San Juan segment of the Caribbean Great Arc can be constrained to approximately 120 Ma. This segment was thus obviously active for more than 65 Ma. An orthogonal convergence rate of 15–25 mm/a requires that a minimum amount of 975–1,625 km of oceanic crust must have been subducted. Both petrological/geochronological data and numerical

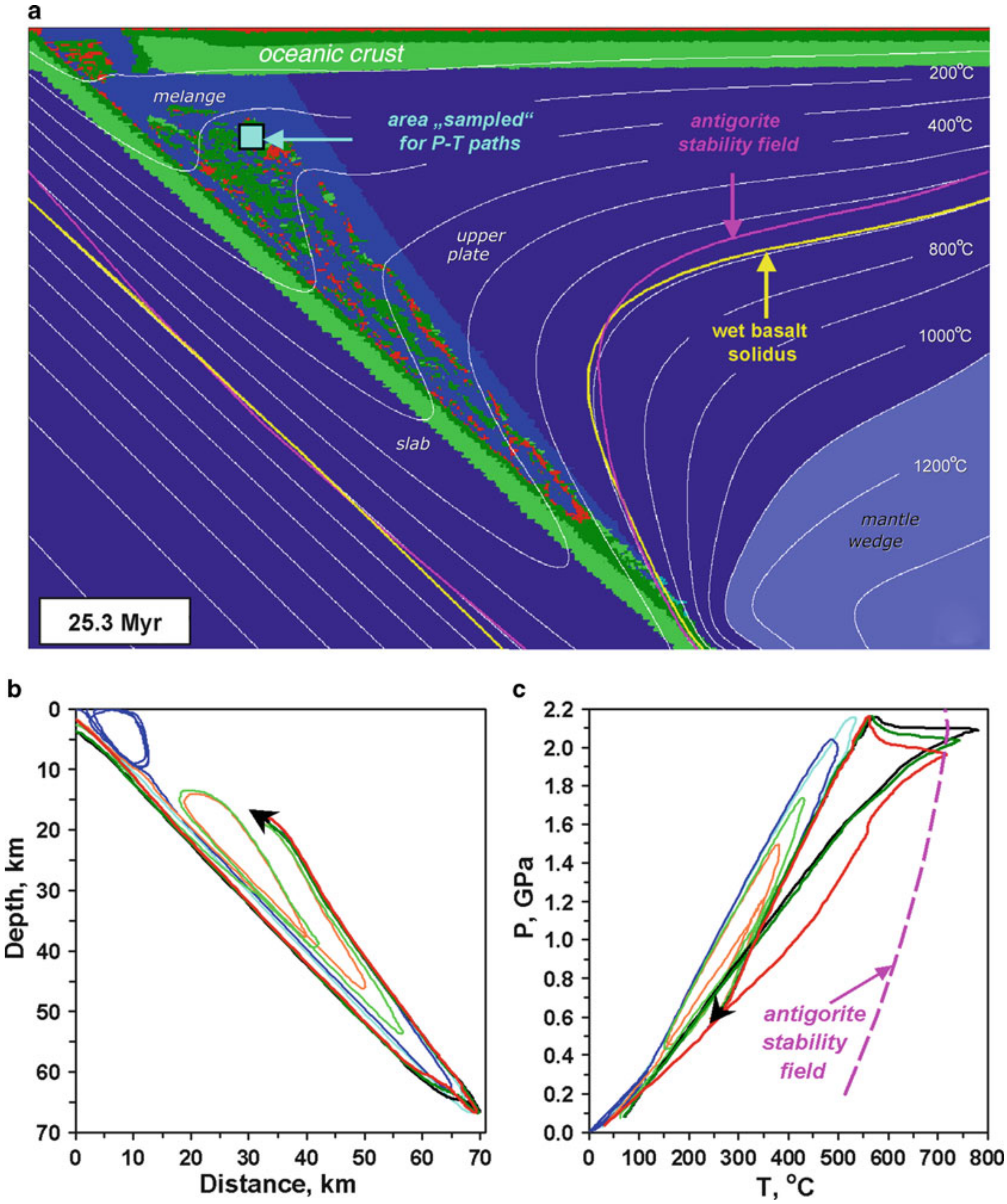

Fig. 2.6 Serpentinite melange (**a**) forming in the spontaneously evolving subduction channel (Fig. 2.6) and characteristic spatial trajectories (**b**) and P–T paths (**c**) of crustal rocks composing the melange. Results from 2D numerical modelling by Gerya et al. (2002).

simulation underscore the broad spectrum of different P–T–time paths and peak conditions recorded by material subducted at different periods of time as the subduction zone evolved and matured.

It has also been shown recently that not only high-pressure eclogites but also ultrahigh-pressure mantle rocks (garnet-bearing peridotites) can be present in intra-oceanic subduction melanges (e.g. in Greater Antilles in Hispaniola, Abbott et al. 2006). Gorczyk et al. (2007a) modelled this phenomenon numerically (Fig. 2.7) and concluded that exhumation of such garnet-bearing peridotites can be related to fore-arc

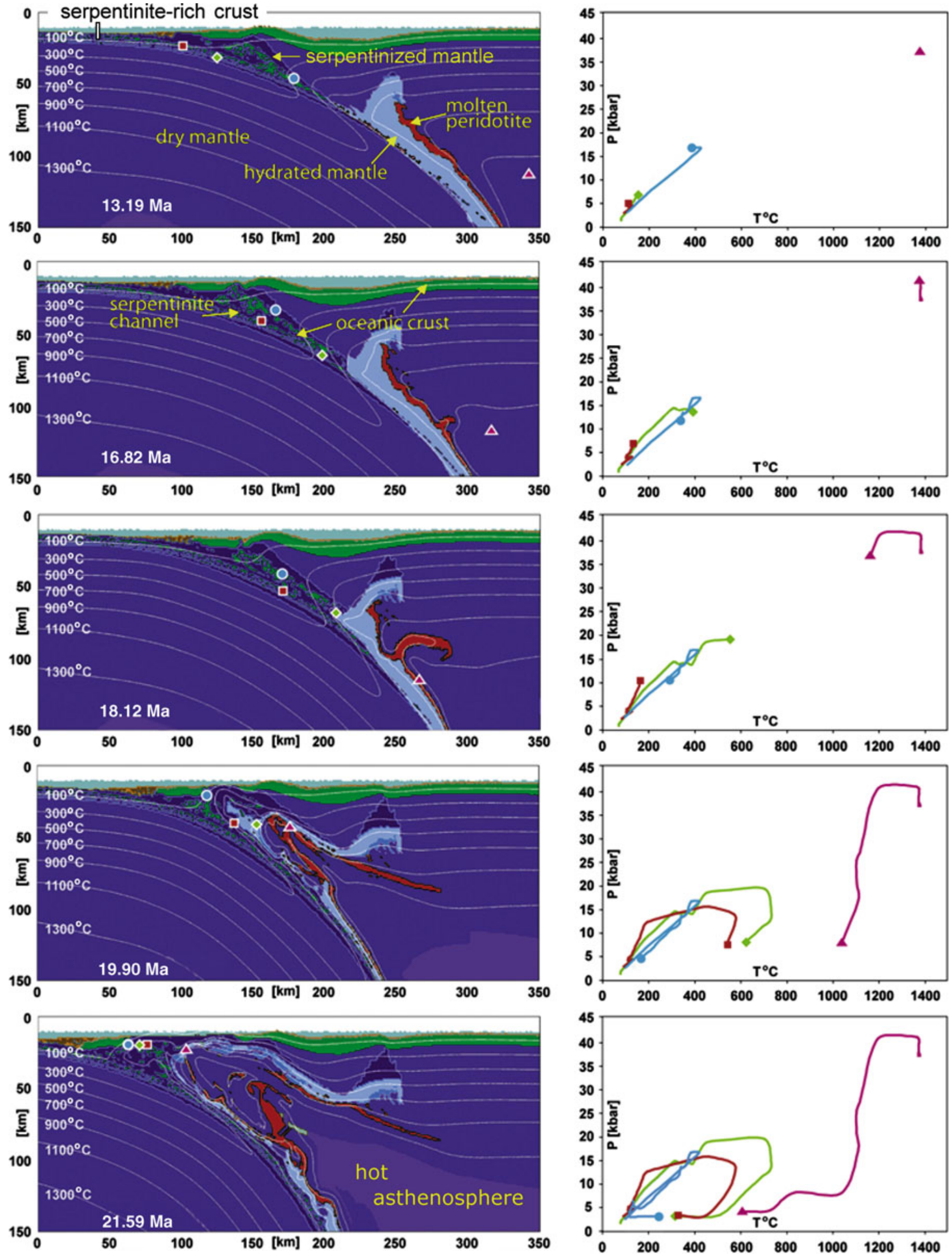

Fig. 2.7 Exhumation of high- and ultrahigh-pressure rocks during retreating intra-oceanic subduction of an oceanic plate originated at slow spreading ridge (left columns) and characteristic P–T paths of crustal and mantle rocks (right column). Results from 2D numerical modelling by Gorczyk et al. (2007a).

extension during subduction of an oceanic plate formed at a slow spreading ridge and characterized by serpentinite-rich crust. In this case subduction channel contains both serpentinites accreted from the subducting plate crust and progressively serpentinized fore-arc mantle. Intense rheological weakening of the mantle wedge takes place due to its strong hydration during subduction of water-rich crust formed at slow spreading ridge. This weakening triggers upwelling of the hydrated peridotites and partially molten peridotites followed by upwelling of hot asthenosphere and subsequent retreat of the subducting slab. According to numerical modelling of P–T paths this process can explain exhumation of UHP rocks in an intra-oceanic setting from depths of up to 120 km (4 GPa).

2.5 Magmatic Crust Growth and Thermal-Chemical Convection in the Mantle Wedge

Reymer and Schubert (1984) estimated rates of crustal generation during intra-oceanic subduction as 20–40 km^3/km/Myr for the western Pacific region based on the total arc crust volume divided by the oldest known igneous age. More recent estimates for the same area by Taira et al. (Izu-Bonin island arc, 1998), Holbrook et al. (Aleutian island arc, 1999) and Dimalanta et al. (Tonga, New Hebrides, Marianas, Southern and Northern Izu-Bonin, Aleutian island arcs, 2002) are somewhat higher, 40–95 km^3/km/Myr and are much higher, 120–180 km^3/km/Myr, according to the work of Stern and Bloomer (early stage of IBM development, 1992). In particular, the arc magmatic addition rate of the arc of the New Hebrides varies between 87 and 95 km^3/km/Myr as determined by Dimalanta et al. (2002). They also give values for addition rates of other island arcs, all of which vary between 30 and 70 km^3/km/Myr. These values are average rates of crust production, calculated by dividing the estimated total volume of produced crust by the time in which it was produced and by the length of the arc.

It is commonly accepted that dehydration of subducting slabs and hydration of the overlying mantle wedges are key processes controlling magmatic activity and consequently crustal growth above subduction zones (e.g., Stern 2002; van Keken et al. 2002; van Keken and King 2005). Mantle wedge processes have been investigated from geophysical (e.g. Zhao et al. 2002; Tamura et al. 2002), numerical (e.g. Davies and Stevenson 1992; Iwamori 1998; Kelemen et al. 2004a; Arcay et al. 2005; Gerya et al. 2006; Nikolaeva et al. 2008), experimental (e.g., Poli and Schmidt 2002; Schmidt and Poli 1998), and geochemical (e.g., Ito and Stern 1986; Sajona et al. 2000; Kelley et al. 2006) perspectives. Indeed, detailed thermal structure and melt production patterns above slabs are still puzzling. Particularly, the relative importance of slab melting (e.g. Kelemen et al. 2004a; Nikolaeva et al. 2008) versus melting induced by simple thermal convection (Honda et al. 2002, 2007; Honda and Saito 2003) and/or thermal-chemical plumes (diapirs) (e.g. Tamura 1994; Hall and Kincaid 2001; Obata and Takazawa 2004; Gerya and Yuen 2003; Manea et al. 2005; Gerya et al. 2006; Gorczyk et al. 2007b; Zhu et al. 2009) to melt production in volcanic arcs is not fully understood.

Several authors (e.g., Tamura et al. 2002; Honda et al. 2007; Zhu et al. 2009) analyzed the spatial distribution of volcanism in Japan and concluded that several clusters of volcanism can be distinguished in space and time (Fig. 2.8). The typical spatial periodicity of such volcanic clusters is 50–100 km (see the spacing between "cigars" in Fig. 2.8b) while their life extent corresponds to 2–7 Myr (see the lengths of "cigars" in time in Fig. 2.8b). Two trench-parallel lines of volcanic density maxima can also be distinguished for some periods of intra-oceanic arc evolution (Fig. 2.8a). Spatial and temporal clustering of volcanic activity also associates with strongly variable (Fig. 4.4 in Calvert 2011) distribution of crustal thickness along intra-oceanic arcs (e.g. Fig. 4.4 in Calvert 2011; Kodaira et al. 2006, 2007) and distribution of seismic velocity anomalies in the mantle wedges under the arcs (e.g. Zhao et al. 1992, 2002; Zhao 2001; Tamura et al. 2002). This further points toward the relations between the mantle wedge processes and crustal growth in intra-oceanic arcs.

Based on 3D numerical models Honda and co-workers (Honda et al. 2002, 2007; Honda and Saito 2003; Honda and Yoshida 2005) proposed the development of small-scale thermally driven convection in the uppermost corner of the mantle wedge with lowered viscosity (low viscosity wedge, LVW, Billen and Gurnis 2001; Conder and Wiens 2007; Honda and Saito 2003; Honda et al. 2002; Honda and Yoshida 2005; Arcay et al. 2005). These authors suggested that

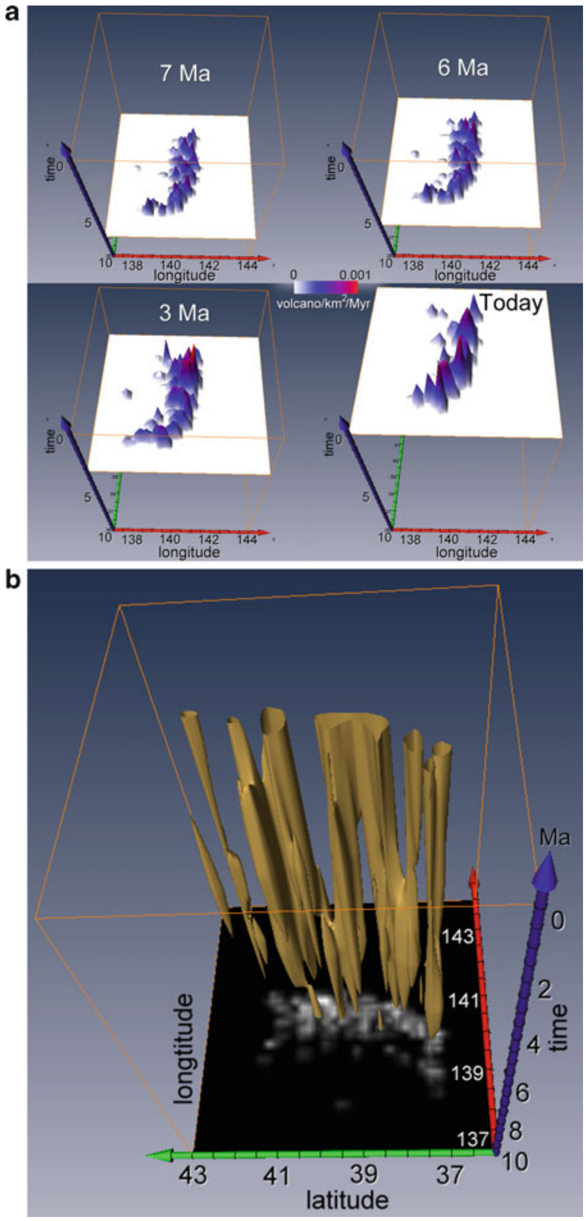

Fig. 2.8 Variations in volcanic activity in NE Japan (Honda and Yoshida 2005; Honda et al. 2007; Zhu et al. 2009). (**a**) variations in the spatial density of volcanoes with their age during the past 10 Myr. (**b**) the isosurface of 0.0003 volcano/km^2/Myr for the observed density of volcanoes in space and time. The density of volcanoes notably evolves showing formation of spatially confined clusters that remain active within certain period of time that could be possibly related to the activity of mantle wedge plumes (cf. Fig. 2.10).

a roll (finger)-like pattern of hot (upwellings) and cold (downwellings) thermal anomalies emerges in the mantle wedge above the subducting slab contributing to clustering of magmatic activity at the arc surface. These purely thermal mantle wedge convection models, however, neglected chemical buoyancy effects coming from hydration and melting atop the subducting slab and leading to thermal-chemical convection and diapirism phenomena (e.g. Tamura 1994; Hall and Kincaid 2001; Gerya and Yuen 2003). These aspects have been recently studied numerically based on petrological-thermomechanical models including water transport and melting. These models predict

1. Spontaneous formation of a low viscosity wedge by hydration of the mantle atop the slab (Arcay et al. 2005; Zhu et al. 2009)
2. Growth of diapiric structures ("cold plumes", Figs. 2.9 and 2.10) above the subducting slab (e.g., Gerya and Yuen 2003; Gorczyk et al. 2007b; Zhu et al. 2009)
3. Broad variation in seismic velocity beneath intraoceanic arcs due to hydration and melting (Gerya et al. 2006; Nakajima and Hasegawa 2003a, b; Gorczyk et al. 2006; Nikolaeva et al. 2008)
4. Variations in melt production and crustal growth processes caused by propagation of hydrated plumes in the mantle wedge (Gorczyk et al. 2007b; Nikolaeva et al. 2008; Zhu et al. 2009)

Nikolaeva et al. (2008) investigated crustal growth processes on the basis of a 2D coupled petrological–thermomechanical numerical model of retreating intraoceanic subduction (Figs. 2.11 and 2.12). The model included spontaneous slab retreat and bending, subducted crust dehydration, aqueous fluid transport, mantle wedge melting, and melt extraction resulting in crustal growth. As follows from the numerical experiments the rate of crust formation is strongly variable with time and positively correlates with subduction rate (Fig. 2.11, bottom diagram). Modelled average rates of crustal growth (30–50 km^3/km/Ma, without effects of dry decompression melting) are close to the lower edge of the observed range of rates for real intraoceanic arcs (40–180 km^3/km/Ma). The composition of new crust depends strongly on the evolution of subduction. Four major magmatic sources can contribute to the formation of the crust: (1) hydrated partially molten peridotite of the mantle wedge, (2) melted subducted sediments, (3) melted subducted basalts, (4) melted subducted gabbro. Crust produced from the first source is always predominant and typically comprise more than 95% of the growing arc crust

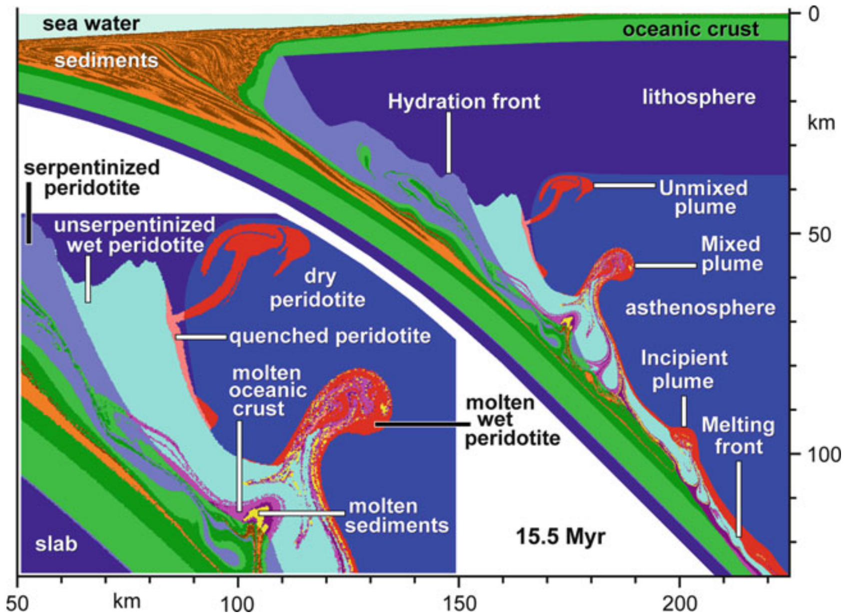

Fig. 2.9 Development of unmixed and mixed plumes due to hydration of the mantle wedge by fluids released from the slab. Plumes rising from the slab are colder then the surrounding mantle wedge (see Fig. 2.10a for 3D thermal structures around such plumes). The corrugations along the hydration front reflect dynamics of slab dehydration controlled by metamorphic reactions. Zoomed area shows lithological structures of mixed and unmixed plumes. Results from 2D numerical modelling by Gerya et al. (2006).

(Nikolaeva et al. 2008). In all studied cases, it appears shortly after beginning of subduction and is a persistent component so long as subduction remains active. Significant amount of crust produced from other three sources appear (1) in the beginning of subduction due to the melting of the slab "nose" and (2) at later stages when subduction velocity is low($<$1 cm/a), which leads to the thermal relaxation of the slab. Both the intensity of melt extraction, and the age of subducted plate affect the volume of new crust. On a long time scale the greatest volume of magmatic arc crust is formed with an intermediate melt extraction threshold (2–6%) and medium subducted plate ages (70–100 Ma) (Nikolaeva et al. 2008).

Recently thermal-chemical mantle wedge convection and related melt production dynamics (Fig. 2.10) were also examined numerically in 3D (Zhu et al. 2009; Honda et al. 2010). Honda et al. (2010) analysed simple subduction model including moderately buoyant chemical agent (water) and found that the hydrated region tends to stay in the corner of the mantle wedge because of its low density and this results in the low temperature zone ("cold nose") there. Moderate chemical buoyancy present in the mantle wedge may either suppress or shift toward the back arc the thermally driven small-scale convection under the arc and make the dominant mantle flow velocity to be normal to the plate boundary. Zhu et al. (2009) examined more complex 3-D petrological-thermomechanical model of intra-oceanic subduction focussing on geometries and patterns of hydrous thermal-chemical upwellings ("cold plumes") formed above the slab (Figs. 2.9 and 2.10). These numerical simulations showed that three types of plumes occur above the slab: (a) finger-like plumes that form sheet-like structure parallel to the trench (Fig. 2.10a, b); (b) ridge-like structures perpendicular to the trench; (c) flattened wave-like instabilities propagating upwards along the upper surface of the slab and forming zig-zag patterns subparallel to the trench.

Zhu et al. (2009) also computed spatial and temporal pattern of melt generation (i.e. crust production) intensity above the slab, which appeared to be strongly controlled by the hydrous plume activities (Fig. 2.10c, d). Peaks of the melt production projected to the arc surface at different moments of time (Fig. 2.10c) always indicate individual thermal-chemical plumes growing at that time. Such peaks often form the linear

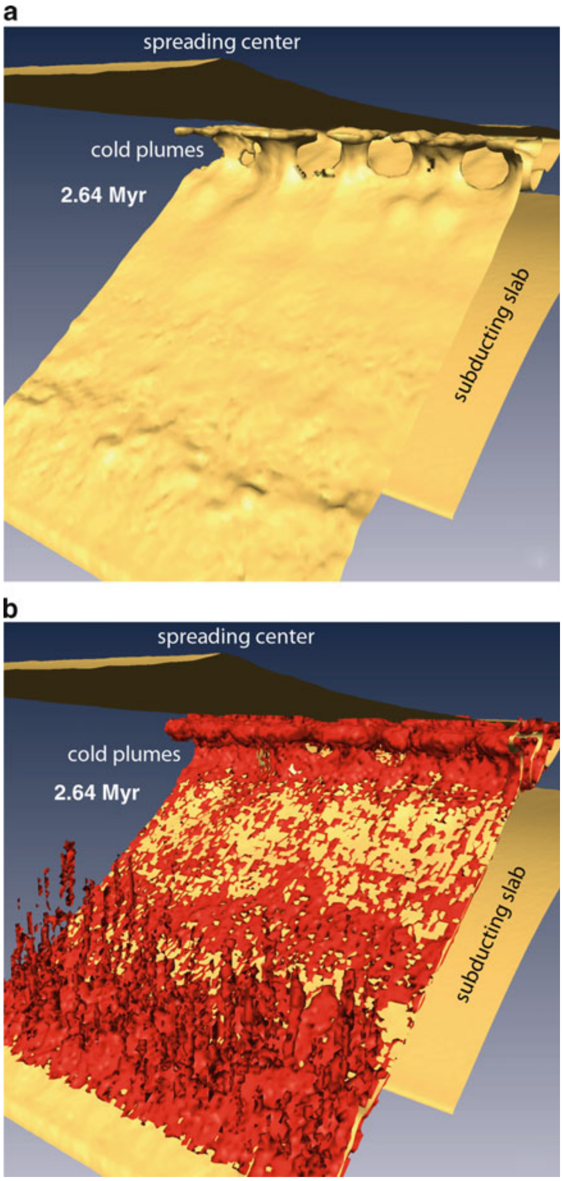

Fig. 2.10 (continued)

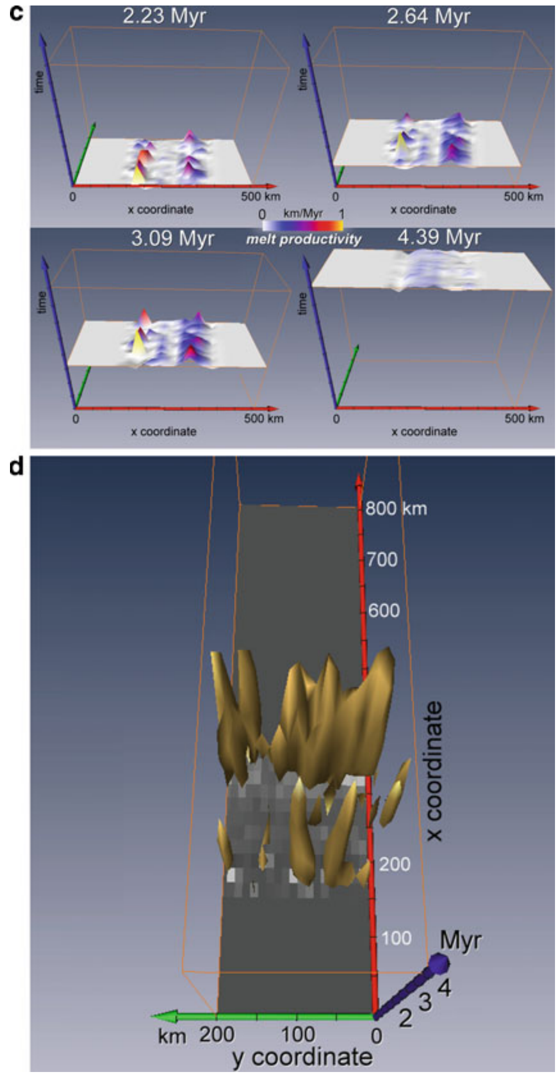

Fig. 2.10 Thermal-chemical plumes (**a**, **b**) growing in the mantle wedge during intra-oceanic subduction and corresponding variations of melt production (**c**, **d**). (**a**) the 1,350 K isosurface of temperature at 2.64 Myr, note that plumes rising from the slab are colder than the surrounding mantle wedge. (**b**) same temperature isosurface (*yellow*) with partially molten rocks, which are responsible for plume buoyancy, shown in *red*. (**c**) variations in the spatial intensity of melt production beneath the surface, peaks in the melt production correspond to individual thermal-chemical plumes shown in (**a**). (**d**) the isosurface of 0.6 $km^3/km^2/Myr$ for melt production, which implies crustal growth intensity of 600 m/Myr. Results from 3D numerical modelling by Zhu et al. (2009).

structure close to the trench, and another line of peaks in linear pattern, which is approximate 200 km away from the trench. The former ones are mainly from the depth of 50–70 km; the latter ones are mainly from the depth of 140–170 km. Figure 2.10d shows the melt productivity in time by visualizing the isosurface (0.6 $km^3/km^2/Myr$) of melt production intensity. The plume-like structures are reflected by distinct “cigar-like” features that are bounded in both time and space (Fig. 2.10d). Each “cigar” corresponds to the activity of a distinct plume that (1) increases the melt productivity during the early stage when the growing melt production is related to decompressing and heating of the rising plume material and (2)

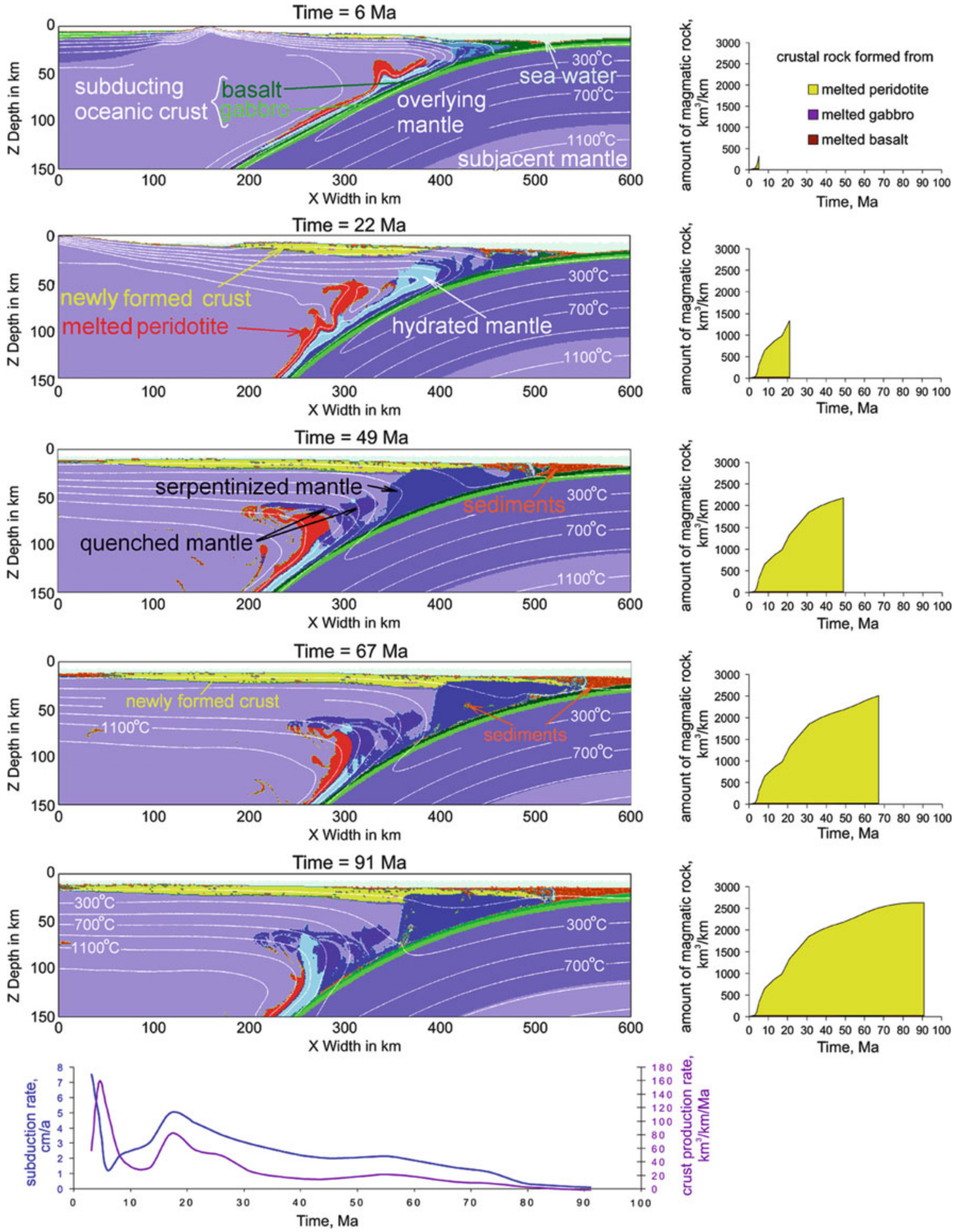

Fig. 2.11 Dynamics of a pure retreating intra-oceanic subduction (left column) and associated magmatic crust growth (right column). Spontaneous changes in subduction rate (for this model subduction rate and trench retreat rate are equal) and crust accumulation rate with time are depicted below. Time is dated from the beginning of subduction. Subduction results in a hydration and partial melting of mantle wedge rocks, which leads to the formation of volcanic arc rocks (*yellow*) above the area of melting. Results from 2D numerical modelling by Nikolaeva et al. (2008).

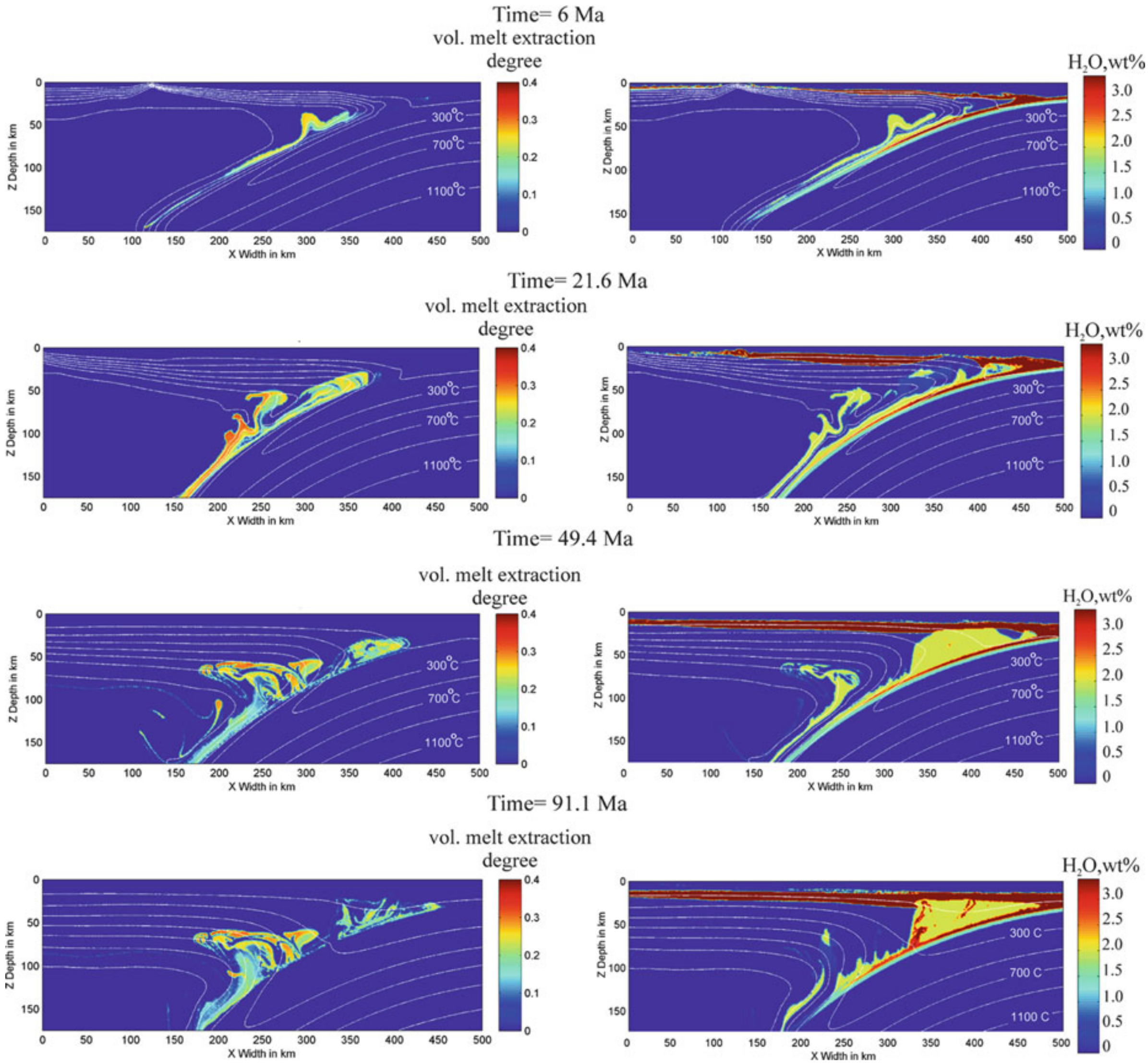

Fig. 2.12 Evolution of degree of melt extraction (left column) and water content (right column) in the mantle wedge and subducting oceanic crust. Corresponding lithological field is depicted on the Fig. 2.11. Results from 2D numerical modelling by Nikolaeva et al. (2008).

decreases the melt productivity during the later stage when the temperature, the pressure and the degree of melting stabilize inside the horizontally spreading and thermally relaxing plume.

The modelled wavelength (25–100 km) and the growth time (2–7 Myr, see the lengths of "cigars" in time in Fig. 2.10d) of the thermal-chemical plumes are comparable to spatial periodicity (50–100 km) and the life extent (2–7 Myr, see the lengths of "cigars" in time in Fig. 2.8b) of volcanic clusters and to spatial periodicity (50–100 km, Fig. 4.4b in Calvert 2011) of crustal thickness variations in intra-oceanic arcs. The existence of two contemporaneous trench-parallel lines of melt productivity (Fig. 2.10b) is also similar to the natural observations (see two trench-parallel lines of Quaternary volcanic density maxima in Fig. 2.8a, at 6 Ma). To explain such phenomena, Wyss et al. (2001) have proposed an additional source of fluids to be located at the top of the slab (at about 150 km depth). Their proposition is based on the velocity tomography in the mantle wedge above the slab, and on the mapping of earthquake size distribution within the mantle wedge. Geochemical evidence (Kimura and Yoshida 2006) for Quaternary lavas from the NE Japan arc also shows the deeper mantle-derived rear-arc lava coming from 100–150 km depth.

2.6 Geochemistry of Intra-oceanic Arcs

The role of subduction zones in global geochemical dynamics is generally twofold: first, crustal materials are recycled back into the deep mantle, and second, new crust is produced in magmatic arcs above subduction zones (e.g. Bourdon et al. 2003). Because the physical and chemical changes within the subducting plate and mantle wedge are largely inaccessible to a direct observation, geochemical investigations concentrate on the input (rocks subducted atop the slabs) and output (magmatic products of island arcs) signals of subduction zones (e.g., Plank and Langmuir 1993; Hauff et al. 2003). For example, as discussed by Kimura and Yoshida (2006), Quaternary lavas from NE Japan arc show geochemical evidence of mixing between mantle-derived basalts and crustal melts at the magmatic front, whereas significant crustal signals are not detected in the rear-arc lavas.

Analyses of comprehensive geochemical data sets for the input and output rock-members (Hauff et al. 2003) from several arc systems such as Aleutian (Yogodzinski et al. 2001), Izu-Bonin-Mariana (Tatsumi et al. 2008), New Britain, Vanuatu (Arai and Ishimaru 2008), Kamchatka (Churikova et al. 2001; Dosseto et al. 2003; Yogodzinski et al. 2001) and Tonga-Kermadec arcs (Turner and Hawkesworth 1997) lead to the conclusion that subduction-related arc basalts (output signal) characteristically have elevated contents of large-ion lithophile element (LILEs) and light rare earth element (LREEs) with depleted heavy REE (HREE) and high field strength elements (HFSEs) compared to subducted crust (input signal) (McCulloch and Gamble 1991; Elliott et al. 1997; Elliott 2003; Plank and Langmuir 1993; Kimura et al. 2009). In relation to that, the following processes are believed to be responsible for the element partitioning in intra-oceanic arc magmas (e.g. Kimura et al. 2009 and reference therein):

- Extraction of fluids and/or melts from the subducted slab; combined slab fluid and melt fluxes may be responsible for geochemical variations along or across magmatic arcs (Eiler et al. 2005; Ishizuka et al. 2006); separate deep and shallow slab components have also been proposed (Kimura and Yoshida 2006; Pearce and Peate 1995; Pearce et al. 2005)
- Fluid fluxed melting of the mantle wedge responsible for generation of high-MgO primitive arc basalts (Arculus and Johnson 1981; Davidson 1996; Elliott et al. 1997; Hawkesworth et al. 1993; Kelemen et al. 1998; Kimura and Yoshida 2006; Plank and Langmuir 1993; Poli and Schmidt 1995; Stern 2002; Stolper and Newman 1994; Tatsumi and Eggins 1995; Turner et al. 1997)
- Slab melt–mantle reaction generating high-MgO primitive arc andesites (Kelemen et al. 2004b; Tatsumi and Hanyu 2003; Tsuchiya et al. 2005; Yogodzinski et al. 1994; Zack et al. 2002)
- Melting of mantle wedge metasomatized by slab-derived fluid or melt (Eiler et al. 2007; Sajona et al. 1996)
- Direct supply of felsic melt from eclogitic slab melting (Defant and Drummond 1990; Martin 1999; Martin et al. 2005)
- Melting of hydrated mantle and subducted tectonic melanges in respectively unmixed and mixed thermal-chemical plumes (Fig. 2.9) rising from the top of the slab (Tamura 1994; Gerya et al. 2006; Castro and Gerya 2008; Castro et al. 2010)

Despite the broad variability of involved geochemical mechanisms currently there is a consensus (e.g. Kimura et al. 2009) about the relative significance of various processes and it is widely believed that slab dehydration or melting combined with the interaction of this slab-derived flux with variously depleted mantle generates primary arc magmas with the observed geochemical characteristics. These primary magmas typically have radiogenic Sr and Pb isotopic composition, with less radiogenic Nd in lavas erupted from the volcanic front compared to rear-arc magmas apparently derived from more depleted upper mantle sources (Elliott et al. 1997; Ishizuka et al. 2003; Kelemen et al. 2004b; Kimura and Yoshida 2006; Manning 2004; Rapp and Watson 1995; Stolper and Newman 1994; Tatsumi and Eggins 1995).

Elliott (2003) and other authors (Hawkesworth et al. 1993; Leat and Larter 2003; McCulloch and Gamble 1991; Stern 2002) describe two distinct major slab components present in arc rocks with different sources and transport mechanisms: (1) melt of the down-going sediments, and (2) aqueous fluid derived from altered oceanic crust. Direct melting of the slab is also suggested as a possible mechanism for melts generation (e.g. Defant and Drummond 1990; Martin 1999; Martin et al. 2005; Kelemen et al. 2004a; Nikolaeva et al. 2008). Fluids and melts liberated from subducting oceanic crust produce melting above slabs and finally lead to efficient subduction-zone arc volcanism (Fig. 2.4). The exact composition of the mobile phases generated in the subducting slab have however, remained incompletely known (e.g. Kessel et al. 2005). In this respect the fundamental control appears to be (e.g. Kimura et al. 2009) the P–T paths of rocks in the subducting slab, which can be approximated by geodynamic modelling (e.g., Peacock and Wang 1999; Gerya and Yuen 2003; Castro and Gerya 2008). For example in the model of Peacock and Wang (1999), subduction of old and cold oceanic plate leads to low slab surface temperature. In contrast, subduction of young and hot oceanic crust typically results in higher slab surface temperatures (Stern et al. 2003).

Such contrasting thermomechanical behaviour can presumably be observed in the arcs of Japan (Peacock and Wang 1999), where the old Pacific Plate (>120 Ma, NE Japan) and the young Shikoku Basin (15–27 Ma, SW Japan) are subducting beneath the Eurasia plate (Kimura and Stern 2009; Kimura et al. 2005; Kimura and Yoshida 2006). Consequently, in NE Japan slab dehydration seems to dominate geochemical signal in the primary arc basalts (Kimura and Yoshida 2006; Moriguti et al. 2004; Shibata and Nakamura 1997), whereas in SW Japan slab melting is proposed to be responsible for generation of high-MgO andesites or adakitic dacites (Kimura and Stern 2009; Kimura et al. 2005; Shimoda and Nohda 1995; Tatsumi and Hanyu 2003). Recently Kimura et al. (2009) obtained similar results from simulations of geochemical variability of primitive magmas across an intra-oceanic arc based on partitioning of incompatible element and Sr-Nd-Pb isotopic composition in a slab-derived fluid and in arc basalt magma generated by an open system fluid-fluxed melting of mantle wedge peridotite (Fig. 2.4). Similar contrasting geochemical behaviour has been also shown (e.g. Kimura et al. 2009 and reference therein) between arcs along the western and eastern Pacific rims. Arc magmatism due to slab-derived fluids is proposed for the western Pacific arcs, including the Kurile, NE Japan, and the Izu-Bonin-Mariana arcs (Ishikawa and Nakamura 1994; Ishikawa and Tera 1999; Ishizuka et al. 2003; Kimura and Yoshida 2006; Moriguti et al. 2004; Pearce et al. 2005; Ryan et al. 1995; Straub and Layne 2003). High-MgO primary mafic magmas from these relatively cold subduction zones show geochemical signatures of extremely fluid mobile elements such as B, Li, or U (Ishikawa and Nakamura 1994; Ishikawa and Tera 1999; Moriguti et al. 2004; Ryan et al. 1995; Turner and Foden 2001). In contrast, slab melting better explains the origin of high-MgO intermediate lavas in the eastern Pacific (Kelemen et al. 2004b; Straub et al. 2008) although the role of slab fluid remains an important factor in some of the arcs (Grove et al. 2006).

Alternative ideas that explain broad variability of slab fluid and slab melt geochemical components in arc magmas were proposed recently based on petrological-thermomechanical numerical modeling of subduction zones (Gerya et al. 2006; Castro and Gerya 2008; Castro et al. 2010). Gerya et al. (2006) suggested that one possibility for transporting two distinct geochemical signatures through the mantle wedge can be related to generation and propagation of partially molten compositionally buoyant diapiric structures (cold plumes, Tamura 1994; Hall and Kincaid 2001; Gerya and Yuen 2003) forming atop the slab. Numerical experiments of Gerya et al. (2006) show that two distinct types of plumes can form in the mantle wedge (Fig. 2.9):

1. Mixed plumes form atop the slab and consist of partially molten mantle and recycled sediments mixed on length-scales of 1–100 m (i.e. subducted tectonic melange). Magma production from such compositionally heterogeneous plumes may produce a strong crustal melt signature in resulting magmas.
2. Unmixed plumes form above the slab and consist of hydrated partially molten mantle located at a distance from the slab, which is therefore not mechanically mixed with subducted crustal rocks. Magma production from such hydrated but compositionally homogeneous plumes may produce a pronounced slab fluid signature.

These distinct plume types can explain the presence of different magmas in volcanic arcs (e.g., Stern 2002): magmas with distinct crustal signatures (e.g., adakites) and primitive magmas from peridotitic source (e.g., arc tholeiites). Thermal zoning inside rapidly rising unmixed cold plumes can result in transient bimodal magmatism because of both the compositional and the thermal zoning of these structures (Fig. 2.10a, b), which would generate basalts from its water-depleted, hot rinds, and boninites from its water-enriched, cooler interiors (Tamura 1994). Rates of plume propagation vary between several centimeters to meters per year (Gerya and Yuen 2003; Gerya et al. 2004) corresponding to 0.1–3 Myr transfer time through the asthenospheric portion of the mantle wedge. This is consistent with U–Th isotope measurements from island arc magmas that suggest short transfer times for fluids (0.03–0.12 Myr) and slab-derived melts (several Myr) (Hawkesworth et al. 1997). It is noteworthy that the diapiric transport (e.g. Tamura 1994; Hall and Kincaid 2001) of various geochemical components in the mantle wedge does not require melting of subducted crust immediately at the slab surface (e.g. Kelemen et al. 2004a). Intense melting of subducted sediments and oceanic crust in the mixed plumes occurs in the temperature range of 900–1,400°C (Gerya and Yuen 2003; Gerya et al. 2006; Castro and Gerya 2008; Castro et al. 2010) after penetration of these structures into the hot portion of the mantle wedge. This behaviour agrees well with geochemical models suggesting notable sediment melting beneath the arc, behaviour which is otherwise not trivial to reconcile (e.g. Kelemen et al. 2004a) with low slab surface temperature inferred from thermal models for subduction zones as discussed by George et al. (2003).

Mixed cold plumes composed of tectonic melanges derived from subduction channels can transport the fertile subducted crustal materials towards hotter zones of the suprasubduction mantle wedge leading to the formation of silicic melts. Recently magmatic consequences of this plausible geodynamic scenario were evaluated by using an experimental approach (Castro and Gerya 2008; Castro et al. 2009, 2010). Melt compositions, fertility and reaction between silicic melts and the peridotite mantle (both hydrous and dry) were tested by means of piston–cylinder experiments at conditions of 1,000°C and pressures of 2.0 and 2.5GPa. The results indicate that silicic melts of trondhjemite and granodiorite compositions may be produced in the ascending mixed plume megastructures. Experiments show that the formation of an Opx-rich reaction band, developed at the contact between the silicic melts and the peridotite, protect silicic melts from further reaction in contrast to the classical view that silicic melts are completely consumed in the mantle. It has also been demonstrated experimentally (Castro et al. 2010) that the composition of melts formed after partial melting of sediment-MORB mélanges is buffered for broad range of sediment-to-MORB ratios (from 3:1 to 1:3), producing liquids along a cotectic of granodiorite to tonalite composition in lower-variance phase assemblage Melt+Grt+Cpx+Pl. The laboratory experiments, therefore, predict decoupling between major element and isotopic compositions: large variations in isotopic ratios can be inherited from a compositionally heterogeneous source but major element compositions can be dependent on the temperature of melting rather than on the composition of the source (Castro et al. 2010).

Important geochemical constrains concerns distribution and amount of water above subduction zones that impose strong controls on chemistry of magmatic arc rocks forming at the surface (e.g., Kelley et al. 2006 and references therein). Flux of water originating from the dehydrating, subducting slab lowers the mantle solidus (e.g., Kushiro et al. 1968) triggering melting of the mantle wedge beneath arcs and back-arc basins (Fig. 2.4). This is supported by a range of various widespread observations on subduction zone lavas (e.g., Kelley et al. 2006 and references therein), seismological data (e.g. Tamura et al. 2002; Jung and Karato 2001; Iwamori 2007) and numerical modelling constrains (Iwamori 1998; Arcay et al. 2005; Nikolaeva et al. 2008; Hebert et al. 2009).

Back-arc basins related to intra-oceanic subduction (Fig. 2.4) are natural places to investigate water-related processes in the mantle wedge because these settings can be treated, in many ways, like mid-ocean ridges (Kelley et al. 2006). Particularly, the driest back-arc basin melts (Fig. 2.13) are compositionally equivalent to mid-ocean ridge melts and can be interpreted as melts generated by decompression melting of ascending mantle (Fig. 2.4). Geochemical studies of back arcs related to intra-oceanic subduction (e.g. Stolper, and Newman 1994; Taylor and Martinez 2003; Kelley et al. 2006) demonstrated the hybrid nature of the back-arc basin melting process:

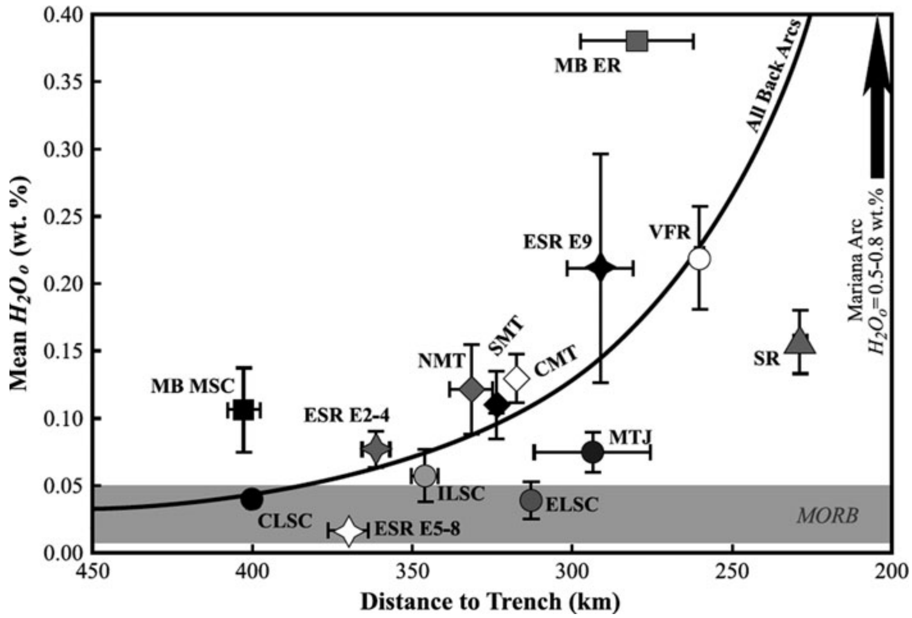

Fig. 2.13 Mean water content in the mantle source (H_2Oo) versus distance to the trench at back-arc basins (Kelley et al. 2006). The back-arc basin data are regional averages of the Manus basin Eastern Rifts (MB ER) and the Manus spreading center/eastern transform zone (MB MSC), the Lau basin central Lau spreading center (CLSC), the intermediate Lau spreading center (ILSC), the Mangatolu triple junction (MTJ), the eastern Lau spreading center (ELSC) and the Valu Fa ridge (VFR), the East Scotia ridge segments (ESR E2–E4, ESR E5–E8, ESR E9), and the Mariana trough northern third (NMT), central third (CMT) and southern third (SMT). The shaded field is the range of H_2Oo for MORB from the same study. The black arrow indicates the direction that volcanic arcs are predicted to plot (Kelley et al. 2006).

MORB-like geochemistry found in relatively dry back-arc melts is systematically perturbed in wetter samples affected by the addition of H_2O-rich material from the subducted slab (Fig. 2.13).

Recently Kelley et al. (2006) examined data compiled from six back-arc basins and three mid-ocean ridge regions and evaluated concentration of H_2O in the mantle source based on measured H_2O concentrations of submarine basalts collected at different distances from the trench (Fig. 2.13). This study clearly demonstrated that water concentrations in back-arc mantle sources increase toward the trench, and back-arc spreading segments with the highest water content are at anomalously shallow water depths, consistent with increases in crustal thickness and total melt production resulting from high H_2O. In contrast to mid ocean ridges, back-arc basin spreading combines ridge-like adiabatic decompression melting with nonadiabatic mantle melting paths that may be independent of the solid flow field and depend on the H_2O supply from the subducting plate (Kelley et al. 2006). This conclusion is also consistent with numerical modelling results (e.g. Iwamori 1998; Arcay et al. 2005; Nikolaeva et al. 2008; Honda et al. 2010) predicting that water-rich mantle sources should mainly concentrate at 100–250 km distances from the trench in proximity of water-rich, depleted and chemically buoyant "cold nose" of the mantle wedge (Figs. 2.11 and 2.12).

2.7 Conclusions

The following messages are "to take home" from this chapter:

- Modern intra-oceanic subduction zones comprise around 40%, of the convergent margins of the Earth and most of them are not accreting sediments and have back-arc extension.
- It is not yet entirely clear where and how intra-oceanic subduction initiates although two major types of subduction zone nucleation scenarios are proposed: induced and spontaneous.

- Internal structure and compositions of intra-oceanic arcs is strongly variable. Both along- and across-arc variation of crustal thickness and lithological structure are inferred based on seismological data and numerical modeling.
- Base of the arc includes crust–mantle transitional layer of partly enigmatic origin (cumulates?, replacive rocks?, intercalation of various rocks and melts?) and imprecisely known thickness.
- Major element composition of magmas feeding arcs from the mantle is debatable, particularly regarding the MgO content of erupted basaltic magmas which are too MgO-poor to represent the parental high-MgO mantle-derived magma. Magma fractionation and reactive flow models are suggested to explain this MgO-paradox.
- Exhumation of high- and ultrahigh-pressure crustal and mantle rocks during intra-oceanic subduction are strongly controlled by serpentinized subduction channels forming by hydration of the overriding plate and incorporation of subducted upper oceanic crust. Newly formed volcanic rocks and depleted mantle from the base of the arc lithosphere can be included into subduction channels at a mature stage of subduction.
- An array of diverse both clockwise and counter clockwise P–T–time paths rather than a single P–T trajectory is characteristic for high-pressure rock melanges forming in the serpentinized channels.
- Crustal growth intensity in intra-oceanic arcs (40–180 km^3/km/Myr) is variable in both space and time and should strongly depend on subduction rate as well as on intensity and character of thermal-chemical convection in the mantle wedge driven by slab dehydration and mantle melting. This convection can possibly include hydrated diapiric structures (cold plumes) rising from the slab and producing silicic magmatic rocks by melting of subducted rock melanges.
- Subduction-related arc basalts (output signal) characteristically have elevated contents of large-ion lithophile element (LILEs) and light rare earth element (LREEs) with depleted heavy REE (HREE) and high field strength elements (HFSEs) compared to subducted oceanic crust (input signal).
- The exact origin of geochemical variations in arc basalts is debatable and may involve a range of processes such as (a) extraction of fluids and/or melts from the subducted slab, (b) fluid fluxed and decompression melting of the mantle wedge, (c) slab melt–mantle reactions, (d) melting of mantle wedge metasomatized by slab-derived fluid or melt, (e) direct supply of felsic melt from eclogitic slab melting, (f) melting of hydrated mantle and subducted tectonic melanges in thermal-chemical plumes.
- Water concentrations in back-arc mantle sources increase toward the trench. Back-arc basin spreading combines mid-ocean-ridge-like adiabatic decompression melting with nonadiabatic fluid-fluxed mantle melting depending on the H_2O supply from the subducting plate. Numerical modeling results predict that water-rich mantle sources should mainly concentrate at 100–250 km distances from the trench in proximity of water-rich, depleted and chemically buoyant „cold nose„ of the mantle wedge.

In conclusion, despite recent progress in both observation and modelling many of the first-order features of intra-oceanic subduction remain only partly known and require further cross-disciplinary efforts.

Acknowledgements This work was supported by ETH Research Grants ETH-0807-2, ETH-0807-3, ETH-0609-2, SNF Research Grants 200020-126832, 200020-129487, SNF ProDoc program 4-D-Adamello and TopoEurope Program.

References

Abbott RN, Draper G, Broman BN (2006) P-T path for ultra-high-pressure garnet ultramafic rocks of the Cuaba Gneiss, Rio San Juan complex, Dominican Republic. Int Geol Rev 48:778–790

Afonso JC, Ranalli G, Fernandez M (2007) Density structure and buoyancy of the oceanic lithosphere revisited. Geophy Res Lett 34, Article Number: L10302

Afonso JC, Zlotnik S, Fernandez M (2008) Effects of compositional and rheological stratifications on small-scale convection under the oceans: implications for the thickness of oceanic lithosphere and seafloor flattening. Geophys Res Lett 35, Article Number: L20308

Alvarez-Marron J, Perez-Estaun A, Danobeitia JJ, Pulgar JA, Martinez Catalan JR, Marcos A, Bastida E, Ayarza Arribas R, Aller J, Gallart A, Gonzalez-Lodeiro E, Banda E, Comas MC, Cordoba D (1996) Seismic structure of the northern continental margin of Spain from ESCIN deep seismic profiles. Tectonophysics 264:153–174

Alvarez-Marron J, Rubio E, Torne M (1997) Subduction-related structures in the North Iberian Margin. J Geophys Res 102:22497–22511

Arai S, Ishimaru S (2008) Insights into petrological characteristics of the lithosphere of mantle wedge beneath arcs through peridotite xenoliths: a review. J Petrol 49:665–695

Arcay D, Tric E, Doin MP (2005) Numerical simulations of subduction zones: effect of slab dehydration on the mantle wedge dynamics. Phys Earth Planet Inter 149:133–153

Arculus RJ, Johnson RW (1981) Island-arc magma sources: a geochemical assessment of the roles of slab derived components and crustal contamination. Geochem J 15:109–133

Billen M, Gurnis M (2001) A low viscosity wedge in subduction zones. Earth Planet Sci Lett 193:227–236

Bourdon B, Turner S, Dosseto A (2003) Dehydration and partial melting in subduction zones: constraints from U-series disequilibria. J Geophys Res 108, Article Number: 2291

Boyd OS, Jones CH, Sheehan AF (2004) Foundering lithosphere imaged beneath the southern Sierra Nevada, California, USA. Science 305:660–662

Burg JP (2011) The Asia-Kohistan-India collision. Review and discussion. In: Brown D, Ryan P (eds) Arc-continent collision: the making of an orogen, Frontiers in earth sciences. Springer, Heidelberg

Burg J-P, Bodinier J-L, Gerya T, Bedini R-M, Boudier F, Dautria J-M, Prikhodko V, Efimov A, Pupier E, Balanec J-L (2009) Translithospheric mantle diapirism: geological evidence and numerical modelling of the Kondyor zoned ultramafic complex (Russian Far-East). J Petrol 50:289–321

Calvert AJ (2011) The seismic structure of island arc crust. In: Brown D, Ryan P (eds) Arc-continent collision: the making of an orogen, Frontiers in earth sciences. Springer, Heidelberg

Casey JF, Dewey JF (1984) Initiation of subduction zones along transforms and accreting plate boundaries, triple junction evolution, and forearc spreading centers: implications for ophiolitic geology and obduction. In: Gass IG, Lippard SJ, Shelton AW (eds) Ophiolites and oceanic lithosphere, vol 13. Geol Soc Spec Publ, London, pp 269–290

Castro A, Gerya TV (2008) Magmatic implications of mantle wedge plumes: experimental study. Lithos 103:138–148

Castro A, García-Casco A, Fernández C, Corretgé LG, Moreno-Ventas I, Gerya T, Löw I (2009) Ordovician ferrosilicic magmas: experimental evidence for ultrahigh temperatures affecting a metagreywacke source. Gondwana Res 16: 622–632

Castro A, Gerya T, Garcia-Casco A, Fernandez C, Diaz-Alvarado J, Moreno-Ventas I, Low I (2010) Melting relations of MORB-sediment melanges in underplated mantle wedge plumes; implications for the origin of Cordilleran-type batholiths. J Petrol 51:1267–1295

Churikova T, Dorendorf F, Worner G (2001) Sources and fluids in the mantle wedge below Kamchatka, evidence from across-arc geochemical variation. J Petrol 42:1567–1593

Cloetingh SAPL, Wortel MJR, Vlaar NJ (1982) Evolution of passive continental margins and initiation of subduction zones. Nature 297:139–142

Cloos M (1982) Flow melanges: numerical modelling and geologic constraints on their origin in the Fransiscan subduction complex, California. Geol Soc Am Bull 93:330–345

Cloos M (1993) Lithospheric buoyancy and collisional orogenesis: subduction of oceanic plateaus, continental margins, island arcs, spreading ridges, and seamounts. Geol Soc Am Bull 105:715–737

Cloos M, Shreve RL (1988a) Subduction-channel model of prism accretion, melange formation, sediment subduction, and subduction erosion at convergent plate margins, 1, Background and description. Pure Appl Geophys 128: 455–500

Cloos M, Shreve RL (1988b) Subduction-channel model of prism accretion, melange formation, sediment subduction, and subduction erosion at convergent plate margins, 2, Implications and discussion. Pure App Geophys 128:501–545

Collins WJ (2003) Slab pull, mantle convection, and Pangaean assembly and dispersal. Earth Planet Sci Lett 205:225–237

Conder JA, Wiens DA (2007) Rapid mantle flow beneath the Tonga volcanic arc. Earth Planet Sci Lett 264:299–307

Conrad WK, Kay RW (1984) Ultramafic and mafic inclusions from Adak Island; crystallization history, and implications for the nature of primary magmas and crustal evolution in the Aleutian arc. J Petrol 25:88–125

Davidson JP (1996) Deciphering mantle and crustal signatures in subduction zone magmatism. In: Bebout GE, Scholl DW, Kirby SH, Platt JR (eds) Subduction top to bottom. American Geophysical Union Monographs, vol 96., pp 251–262

Davies GF (1999) Dynamic Earth. Cambridge University Press, New York

Davies JH, Stevenson DJ (1992) Physical model of source region of subduction zone volcanics. J Geophys Res 97: 2037–2070

Defant MJ, Drummond MS (1990) Derivation of some modern arc magmas by melting of young subducted lithosphere. Nature 347:662–665

Dewey JF (1969) Continental margins: a model for conversion of Atlantic type to Andean type. Earth Planet Sci Lett 6: 189–197

Dickinson WR, Seely DR (1979) Structure and stratigraphy of fore-arc regions. Am Assoc Petrol Geol Bull 63:2–31

Dimalanta C, Taira A, Yumul GP, Tokuyama H, Mochizuki K (2002) New rates of western Pacific island arc magmatism from seismic and gravity data. Earth Planet Sci Lett 202: 105–115

Doin M-P, Henry P (2001) Subduction initiation and continental crust recycling: the roles of rheology and eclogitization. Tectonophysics 342:163–191

Dosseto A, Bourdon B, Joron J-L, Dupre B (2003) U-Th-Pa-Ra study of the Kamchatka arc: new constraints on the genesis of arc lavas. Geochem Cosmochem Acta 67:2857–2877

Eiler JM, Carr MJ, Reagan M, Stolper EM (2005) Oxygen isotope constraints on the sources of Central American arc lavas. Geochem Geophys Geosyst 6, Article Number: Q07007

Eiler JM, Schiano P, Valley JM, Kita NT, Stolper EM (2007) Oxygen-isotope and trace element constraints on the origins of silica-rich melts in the subarc mantle. Geochem Geophys Geosyst 8, Article Number: Q09012

Elliott T (2003) Tracers of the slab. In: Eiler J (ed) Inside the subduction factory. American Geophysical Union, Washington, DC, pp 23–46

Elliott T, Plank T, Zindler A, White W, Bourdon B (1997) Element transport from slab to volcanic front at the Mariana arc. J Geophys Res 102:14991–15019

Erickson SG (1993) Sedimentary loading, lithospheric flexure, and subduction initiation at passive margins. Geology 21: 125–128

Ernst WG (1977) Mineral parageneses and plate tectonic settings of relatively high-pressure metamorphic belts. Fortschr Miner 54:192–222

Federico L, Crispini L, Scambelluri M, Capponi G (2007) Ophiolite mélange zone records exhumation in a fossil subduction channel. Geology 35:499–502

Fyfe WS, Leonardos OH (1977) Speculations on causes of crustal rifting and subduction, with applications to Atlantic margin of Brazil. Tectonophysics 42(1):29–36

George R, Turner S, Hawkesworth C, Morris J, Nye C, Ryan J, Zheng S-H (2003) Melting processes and fluid and sediment transport rates along the Alaska-Aleutian arc from an integrated U-Th-Ra-Be isotope study. J Geophys Res 108, doi:10.1029/2002JB001916

Gerya TV, Burg J-P (2007) Intrusion of ultramafic magmatic bodies into the continental crust: numerical simulation. PEPI 160:124–142

Gerya TV, Meilick FI (2011) Geodynamic regimes of subduction under an active margin: effects of rheological weakening by fluids and melts. J Metamorphic Geol 29:7–31

Gerya TV, Yuen DA (2003) Rayleigh-Taylor instabilities from hydration and melting propel "cold plumes" at subduction zones. Earth Planet Sci Lett 212:47–62

Gerya TV, Stoeckhert B, Perchuk AL (2002) Exhumation of high-pressure metamorphic rocks in a subduction channel – a numerical simulation. Tectonics 21, Article Number: 1056

Gerya TV, Yuen DA, Sevre EOD (2004) Dynamical causes for incipient magma chambers above slabs. Geology 32:89–92

Gerya TV, Connolly JAD, Yuen DA, Gorczyk W, Capel AM (2006) Sesmic implications of mantle wedge plumes. Phys Earth Planet Inter 156:59–74

Gerya TV, Connolly JAD, Yuen DA (2008) Why is terrestrial subduction one-sided? Geology 36:43–46

Gorczyk W, Gerya TV, Connolly JAD, Yuen DA, Rudolph M (2006) Large-scale rigid-body rotation in the mantle wedge and its implications for seismic tomography. Geochem Geophys Geosyst 7, Article Number: Q05018

Gorczyk W, Guillot S, Gerya TV, Hattori K (2007a) Asthenospheric upwelling, oceanic slab retreat, and exhumation of UHP mantle rocks: insights from Greater Antilles. Geophys Res Lett 34, Article Number: L21309

Gorczyk W, Gerya TV, Connolly JAD, Yuen DA (2007b) Growth and mixing dynamics of mantle wedge plumes. Geology 35:587–590

Goren L, Aharonov E, Mulugeta G, Koyi HA, Mart Y (2008) Ductile deformation of passive margins: a new mechanism for subduction initiation. J Geophys Res 113, Article Number: B08411

Grove TL, Chatterjee N, Parman SW, Medard E (2006) The influence of H2O on mantle wedge melting. Earth Planet Sci Lett 249:74–89

Gurnis M, Hall C, Lavier L (2004) Evolving force balance during incipient subduction. Geochem Geophys Geosyst 5, Article Number Q07001

Hall PS, Kincaid C (2001) Diapiric flow at subduction zones: a recipe for rapid transport. Science 292:2472–2475

Hall C, Gurnis M, Sdrolias M, Lavier LL, Müller RD (2003) Catastrophic initiation of subduction following forced convergence across fracture zones, Earth Planet. Sci Lett 212: 15–30

Hauff F, Hoernle K, Schmidt A (2003) Sr-Nd-Pb composition of Mesozoic Pacific oceanic crust (Site 1149 and 801, ODP Leg 185): implications for alteration of ocean crust and the input into the Izu-Bonin-Mariana subduction system. Geochem Geophys Geosyst 4, Article Number: 8913

Hawkesworth CJ, Gallagher K, Hergt JM, McDermott F (1993) Trace element fractionation processes in the generation of island arc basalts. Philos Trans R Soc London Ser A 342: 179–191

Hawkesworth CJ, Turner SP, McDermott F, Peate DW, van Calsteren P (1997) U-Th isotopes in arc magmas: implications for element transfer from the subducted crust. Science 276:551–555

Hebert LB, Antoshechkina P, Asimow P, Gurnis M (2009) Emergence of a low-viscosity channel in subduction zones through the coupling of mantle flow and thermodynamics, Earth Planet. Sci Lett 278:243–256

Hermann J, Muntener O, Scambelluri M (2000) The importance of serpentinite mylonites for subduction and exhumation of oceanic crust. Tectonophysics 327:225–238

Hilde TWE, Uyeda S, Kroenke L (1976) Evolution of the western Pacific and its margin. Tectonophysics 38: 145–165

Holbrook WS, Lizarralde D, McGeary S, Bangs N, Diebold J (1999) Structure and composition of Aleutian island arc and implications for continental crustal growth. Geology 27: 31–34

Honda S, Saito M (2003) Small-scale convection under the back-arc occurring in the low viscosity wedge, Earth Planet. Sci Lett 216:703–715

Honda S, Yoshida T (2005) Application of the model of small-scale convection under the island arc to the NE Honshu subduction zone. Geochem Geophys Geosyst 6, Article Number: Q06004

Honda S, Saito M, Nakakuki T (2002) Possible existence of small-scale convection under the back arc. Geophys Res Lett 29:20–43

Honda S, Yoshida T, Aoike K (2007) Spatial and temporal evolution of arc volcanism in the northeast Honshu and Izu-Bonin arcs: evidence of small-scale convection under the island arc? Isl Arc 16:214–223

Honda S, Gerya T, Zhu G (2010) A simple three-dimensional model of thermo–chemical convection in the mantle wedge. Earth Planet Sci Lett 290:311–318

Hsu KJ (1971) Franciscan melange as a model for eugeosunclinal sedimentation and underthrusting tectonics. J Geophys Res 76:1162–1170

Ishikawa T, Nakamura E (1994) Origin of the slab component in arc lavas from across-arc variation of B and Pb isotopes. Nature 370:205–208

Ishikawa T, Tera F (1999) Two isotopically distinct fluid components involved in the Mariana Arc: evidence from Nb/B ratios and B, Sr, Nd, and Pb isotope systematic. Geology 27:83–86

Ishizuka O, Taylor RN, Milton JA, Nesbitt RW (2003) Fluid-mantle interaction in an intra-oceanic arc: constraints from high-precision Pb isotopes, Earth Planet. Sci Lett 211: 221–236

Ishizuka O, Taylor RN, Milton JA, Nesbitt RE, Yuasa M, Sakamoto I (2006) Variation in the mantle sources of the northern Izu arc with time and space – Constraints from high-precision Pb isotopes. J Volcanol Geotherm Res 156: 266–290

Ito E, Stern RJ (1986) Oxygen-isotopic and strontium isotopic investigations of subduction zone volcanism – the case of the Volcano Arc and the Marianas Island-Arc. Earth Planet Sci Lett 76:312–320

Iwamori H (1998) Transportation of H2O and melting in subduction zones, Earth Planet. Sci Lett 160:65–80

Iwamori H (2007) Transportation of H2O beneath the Japan arcs and its implications for global water circulation. Chem Geol 239:182–198

Jagoutz O, Müntener O, Burg J-P, Ulmer P, Jagoutz E (2006) Lower continental crust formation through focused flow in km-scale melt conduits: the zoned ultramafic bodies of the Chilas Complex in the Kohistan island arc (NW Pakistan). Earth Planet Sci Lett 242:320–342

Jull M, Kelemen PB (2001) On the conditions for lower crustal convective instability, J. Geophys. Res., B. Solid Earth Planets 106:6423–6446

Jung H, Karato S (2001) Water-induced fabric transitions in olivine. Science 293:1460–1463

Karig DE (1982) Initiation of subduction zones: implications for arc evolution and ophiolite development. Geol Soc Lond Spec Pub 10:563–576

Karson J, Dewey JF (1978) Coastal Complex, western Newfoundland: an early Ordovician oceanic fracture zone. BullGeol Soc Amer 89:1037–1049

Kay SM, Kay RW (1985) Aleutian tholeiitic and calc-alkaline magma series: 1. The mafic phenocrysts. Contrib Mineral Petrol 90:276–290

Kay SM, Kay RW (1991) Creation and destruction of lower continental crust. In: Stoeckhert B, Wedepohl KH (eds) Crustal dynamics; pathways and records, International Journal of Earth Sciences, vol 80, 2, Springer, Berlin, pp 259–278

Kay SM, Kay RW (1993) Delamination and delamination magmatism. In: Green AG, Kroener A, Goetze HJ, Pavlenkova N (eds) New horizons in strong motion; seismic studies and engineering practice, Tectonophysics, vol 219, 1–3, Elsevier, Amsterdam, Netherlands, pp 177–189

Kelemen PB, Hart SR, Bernstein S (1998) Silica enrichment in the continental upper mantle via melt/rock reaction. Earth Planet Sci Lett 164:387–406

Kelemen P, Hanghoj K, Greene A (2003) One view of the geochemistry of subduction-related magmatic arcs, with an emphasis on primitive andesite and lower crust. In: Rudnick RL (ed) The crust, treatise on geochemistry, vol 3. Elsevier Pergamon, Oxford, pp 593–659

Kelemen PB, Rilling JL, Parmentier EM, Mehl L, Hacker BR (2004a) Thermal structure due to solid-state flow in the mantle wedge beneath arcs. In: Eiler JM (ed) Inside the subduction factory, vol 138, Geophys Monogr Ser. AGU, Washington, DC, pp 293–311

Kelemen PB, Yogodzinski GM, Scholl DW (2004b) Along-strike variation in the Aleutian island arc: genesis of high Mg# andesite and implications for continental crust. In: Eiler JM (ed) Inside the subduction factory, vol 138, Geophys Monogr Ser. AGU, Washington, DC, pp 223–276

Kelley KA, Plank T, Grove TL, Stolper EM, Newman S, Hauri E (2006) Mantle melting as a function of water content beneath back-arc basins. J Geophys Res 111, Article Number: B09208

Kemp DV, Stevenson DJ (1996) A tensile, flexural model for the initiation of subduction. Geophys J Int 125:73–94

Kessel R, Schmidt MW, Pettke T, Ulmer P (2005) The trace element signature of subduction zone fluids, melts, and supercritical liquids at 120–180 km depth. Nature 437:724–727

Kimura J-I, Stern RJ (2009) Neogene volcanism of the Japan island arc: the K-h relationship revisited. In: Circum pacific tectonics, geologic evolution, and ore deposits. Arizona Geological Society Digest, Arizona Geological Society, Tucson, vol 22, pp 187–202

Kimura J, Yoshida T (2006) Contributions of slab fluid, mantle wedge and crust to the origin of quaternary lavas in the NE Japan arc. J Petrol 47:2185–2232

Kimura J-I, Stern RJ, Yoshida T (2005) Re-initiation of subduction and magmatic responses in SW Japan during Neogene time. Geol Soc Am Bull 117:969–986

Kimura J-I, Hacker B.R, van Keken PE, Kawabata H,Yoshida T, Stern RJ (2009) Arc basalt simulator version 2, a simulation for slab dehydration and fluid-fluxed mantle melting for arc basalts: modeling scheme and application. Geochem Geophys Geosyst 10, Article Number: Q09004

Kodaira S, Sato T, Takahashi N, Ito A, Tamura Y, Tatsumi Y, Kaneda Y (2006) Seismological evidence for variable growth of crust along the Izu intraoceanic arc. J Geophys Res 112, Article Number: B05104

Kodaira S, Sato T, Takahashi N, Miura S, Tamura Y, Tatsumi Y, Kaneda Y (2007) New seismological constraints on growth of continental crust in the Izu-Bonin intra-oceanic arc. Geology 35:1031–1034

Kodaira S, Sato T, Takahashi N, Yamashita M, No T, Kaneda Y (2008) Seismic imaging of a possible paleoarc in the Izu-Bonin intraoceanic arc and its implications for arc evolution processes. Geochem Geophys Geosyst 9, Article Number: Q10X01

Krebs M, Maresch WV, Schertl H-P, Münker C, Baumann A, Draper G, Idleman B, Trapp E (2008) The dynamics of intra-oceanic subduction zones: a direct comparison between fossil petrological evidence (Rio San Juan Complex, Dominican Republic) and numerical simulation. Lithos 103:106–137

Kushiro I, Syono Y, Akimoto S (1968) Melting of a peridotite nodule at high pressures and high water pressures. J Geophys Res 73:6023–6029

Leat PT, Larter RD (2003) Intra-oceanic subduction systems: introduction. In: Larter RD, Leat PT (eds) Intra-oceanic subduction systems: tectonic and magmatic processes, vol 219. Geological Society of London, Special Publications, London, pp 1–17

Leat PT, Riley TR, Wareham CD, Millar IL, Kelley SP, Storey BC (2002) Tectonic setting of primitive magmas in volcanic arcs: an example from the Antarctic Peninsula. J Geol Soc Lond 159:31–44

Manea VC, Manea M, Kostoglodov V, Sewell G (2005) Thermo-mechanical model of the mantle wedge in Central Mexican subduction zone and a blob tracing approach for the magma transport. Phys Earth Planet Inter 149:165–186

Manning CE (2004) The chemistry of subduction-zone fluids. Earth Planet Sci Lett 223:1–16

Marques FO, Gerya T, Nikolaeva K (2008) Subduction initiation at a passive margin: a prototype candidate. 33rd IGC, Abstract Volume, Oslo, Norway

Mart Y, Aharonov E, Mulugeta G, Ryan W, Tentler T, Goren L (2005) Analogue modelling of the initiation of subduction. Geophys J Int 160:1081–1091

Martin H (1999) Adakitic magmas: modern analogues of Archaean granitoids. Lithos 46:411–429

Martin H, Smithies RH, Rapp R, Moyen J-F, Champion D (2005) An overview of adakite, tonalite-trondhjemite-granodiorite (TTG), and sanukitoid: relationships and some implications for crustal evolution. Lithos 79:1–24

Maruyama S, Liou JG, Terabayashi M (1996) Blueschists and eclogites in the world and their exhumation. Int Geol Rev 38:485–594

Masson DG, Cartwright JA, Pinheiro LM, Whitmarsh RB, Beslier M-O, Roeser H (1994) Compressional deformation at the ocean–continent transition in the NE Atlantic. J Geol Soc London 151:607–613

McCulloch MT, Gamble JA (1991) Geochemical and geodynamical constraints on subduction zone magmatism. Earth Planet Sci Lett 102:358–374

McKenzie DP (1977) The initiation of trenches: a finite amplitude instability. In: Talwani M, Pitman WC III (eds) Island arcs, deep sea trenches and back-arc basins, vol 1, Maurice Ewing Series. AGU, Washington, DC, pp 57–61

Mitchell AHG (1984) Initiation of subduction of post-collision foreland thrusting and back-thrusting. J Geodyn 1:103–120

Moriguti T, Shibata T, Nakamura E (2004) Lithium, boron and lead isotope and trace element systematics of Quaternary basaltic volcanic rocks in northeastern Japan: mineralogical controls on slab-derived fluid composition. Chem Geol 212:81–100

Müeller S, Phillips RJ (1991) On the initiation of subduction. J Geophys Res 96:651–665

Müntener O, Kelemen PB, Grove TL (2001) The role of H2O during crystallization of primitive arc magmas under uppermost mantle conditions and genesis of igneous pyroxenites; an experimental study. Contrib Mineral Petrol 141:643–658

Nakajima J, Hasegawa A (2003a) Estimation of thermal structure in the mantle wedge of northeastern Japan from seismic attenuation data. Geophys Res Lett 30, Article Number: 1760

Nakajima J, Hasegawa A (2003b) Tomographic imaging of seismic velocity structure in and around the Onikobe volcanic area, northeastern Japan: implications for fluid distribution. J Volcanol Geotherm Res 127:1–18

Nikolaeva K, Gerya TV, Connolly JAD (2008) Numerical modelling of crustal growth in intraoceanic volcanic arcs. Phys Earth Planet Inter 171:336–356

Nikolaeva K, Gerya TV, Marques FO (2010) Subduction initiation at passive margins: numerical modeling. J Geophys Res 115, Article Number: B03406

Niu Y, O'Hara MJ, Pearce JA (2003) Initiation of subduction zones as a consequence of lateral compositional buoyancy contrast within the lithosphere: a petrological perspective. J Petrol 44(5):851–866

Obata M, Takazawa E (2004) Compositional continuity and discontinuity in the Horoman peridotite, Japan, and its implication for melt extraction processes in partially molten upper mantle. J Petrol 45:223–234

Oxburg ER, Parmentier EM (1977) Compositional and density stratification in oceanic lithosphere – causes and consequences. J Geol Soc London 133:343–355

Pascal C, Cloetingh SAPL (2009) Gravitational potential stresses and stress field of passive continental margins: insights from the south-Norway shelf. Earth Planet Sci Lett 277:464–473

Peacock SM, Wang K (1999) Seismic consequence of warm versus cool subduction metamorphism: examples from southwest and northeast Japan. Science 286:937–939

Pearce JA, Peate DW (1995) Tectonic implications of the composition of volcanic arc magmas. Annu Rev Earth Planet Sci 23:251–285

Pearce JA, Stern RJ, Bloomer SH, Fryer P (2005) Geochemical mapping of the Mariana arc-basin system: implications for the nature and distribution of subduction components. Geochem Geophys Geosyst 6, Article Number: Q07006

Pichavant M, Macdonald R (2003) Mantle genesis and crustal evolution of primitive calc-alkaline basaltic liquids from the Lesser Antilles arc. In: Larter RD, Leat PT (eds) Intra-oceanic Subduction Systems: Tectonic and Magmatic Processes, vol 219. Geological Society of London, Special Publications, London, pp 239–254

Plank T, Langmuir CH (1993) Tracing trace-elements from sediment input to volcanic output at Subduction Zones. Nature 362:739–743

Platt JP (1993) Exhumation of high-pressure rocks: a review of concepts and processes. Terra Nova 5:119–133

Poli S, Schmidt MW (1995) H2O transport and release in subduction zones: experimental constraints on basaltic and andesitic systems. J Geophys Res 100:22299–22314

Poli S, Schmidt MW (2002) Petrology of subducted slabs. Annu Rev Earth Planet Sci 30:207–235

Pysklywec RN, Mitrovica JX, Ishii M (2003) Mantle avalanche as a driving force for tectonic reorganization in the southwest Pacific. Earth Planet Sci Lett 209:29–38

Rapp EP, Watson EB (1995) Dehydration melting of metabasalt at 8–32 kbar: implications for continental growth and crustal-mantle recycling. J Petrol 36:891–931

Regenauer-Lieb K, Yuen DA, Branlund J (2001) The initiation of subduction: critically by addition of water? Science 294: 578–580

Reymer A, Schubert G (1984) Phanerozoic addition rates to the continental crust and crustal growth. Tectonics 3:63–77

Ring U, Brandon MT, Willett SD, Lister GS (1999) Exhumation processes. In: Ring U, Brandon MT, Lister GS, Willett SD (eds) Exhumation processes: normal faulting, ductile flow, and erosion, Geological Society, London, Special Publications, 154, pp 1–27

Rudnick RL, Gao S (2003) The composition of the continental crust. In: Rudnick RL (ed) The crust, treatise on geochemistry, vol 3. Elsevier, Oxford, pp 1–64

Ryan JG, Morris J, Tera F, Leeman WP, Tsvetkov A (1995) Cross-arc geochemical variations in the Kurile Arc as a function of slab depth. Science 270:625–627

Sajona FG, Maury RC, Bellon H, Cotten J, Defant M (1996) High field strength element enrichment of Pliocene-Pleistocene island arc basalts, Zamboanga Peninsula, western Mindanao (Philippines). J Petrol 37:693–726

Sajona FG, Maury RC, Prouteau G, Cotten J, Schiano P, Bellon H, Fontaine L (2000) Slab melt as metasomatic agent in island arc magma mantle sources, Negros and Batan (Philippines). Isl Arc 9:472–486

Schellart WP, Freeman J, Stegman DR, Moresi L, May D (2007) Evolution and diversity of subduction zones controlled by slab width. Nature 446:308

Schmidt MW, Poli S (1998) Experimentally based water budgets for dehydrating slabs and consequences for arc magma generation. Earth Planet Sci Lett 163:361–379

Shibata T, Nakamura E (1997) Across-arc variations of isotope and trace element compositions from Quaternary basaltic rocks in northeastern Japan: implications for interaction between subducted oceanic slab and mantle wedge. J Geophys Res 102:8051–8064

Shimoda G, Nohda S (1995) Lead isotope analyses: an application to GSJ standard rock samples. Human Environ Stud 4:29–36

Shreve RL, Cloos M (1986) Dynamics of sediment subduction, melange formation, and prism accretion. J Geophys Res 91:10229–10245

Sizova E, Gerya T, Brown M, Perchuk LL (2009) Subduction styles in the Precambrian: insight from numerical experiments. Lithos. doi:10.1016/j.lithos.2009.05.028

Smith IEM, Worthington TJ, Price RC, Gamble JA (1997) Primitive magmas in arc-type volcanic associations: examples from the southwest Pacific. Can Mineral 35:257–273

Solomatov VS (2004) Initiation of subduction by small-scale convection. J Geophys Res 109, Article Number: B05408

Stern RJ (2002) Subduction zones. Rev Geophys 40:3-1–3-38

Stern RJ (2004) Subduction initiation: spontaneous and induced. Earth Planet Sci Lett 226:275–292

Stern RJ, Bloomer SH (1992) Subduction zone infancy: examples from the Eocene Izu-Bonin-Mariana and Jurassic California arcs. Geol Soc Am Bull 104:1621–1636

Stern RJ, Fouch MJ, Klemperer SL (2003) An overview of the Izu-Bonin-Mariana subduction factory. In: Eiler J (ed) Inside the subduction factory, vol 138, Geophys Monogr Ser. AGU, Washington, DC, pp 175–222

Stolper E, Newman S (1994) The role of water in the petrogenesis of Mariana trough magmas, Earth Planet. Sci Lett 121:293–325

Straub SM, Layne GD (2003) The systematic of chlorine, fluorine, and water in Izu arc front volcanic rocks: implications for volatile recycling in subduction zones. Geochim Cosmochim Acta 67:4179–4203

Straub SM, LaGatta AB, Martin-DelPozzo AL, Langmuir CH (2008) Evidence from high-Ni olivines for a hybridized peridotite/pyroxenite source for orogenic andesites from the central Mexican Volcanic Belt. Geochem Geophys Geosyst 9, Article Number: Q03007

Taira A, Saito S, Aoike K, Morita S, Tokuyama H, Suyehiro K, Takahashi N, Shinohara M, Kiyokawa S, Naka J, Klaus A (1998) Nature and growth rate of the Northern Izu-Bonin (Ogasawara) arc crust and their implications for continental crust formation. Isl Arc 7:395–407

Takahashi N, Kodaira S, Klemperer SL, Tatsumi Y, Kaneda Y, Suyehiro K (2007) Crustal structure and evolution of the Mariana intra-oceanic island arc. Geology 35:203–206

Takahashi N, Kodaira S, Tatsumi Y, Yamashita M, Sato T, Kaiho Y, Miura S, No T, Takizawa K, Kaneda Y (2009) Structural variations of arc crusts and rifted margins in the southern Izu-Ogasawara arc-back arc system. Geochem Geophys Geosyst 10, Article Number: Q09X08

Tamura Y (1994) Genesis of island arc magmas by mantle derived bimodal magmatism: evidence from the Shirahama Group. Jpn: J Petrol 35:619–645

Tamura Y, Tatsumi Y, Zhao DP, Kido Y, Shukuno H (2002) Hot fingers in the mantle wedge: new insights into magma genesis in subduction zones. Earth Planet Sci Lett 197: 105–116

Tatsumi Y, Eggins S (1995) Subduction-zone magmatism. Blackwell Science, Cambridge, MA, 211 pp

Tatsumi Y, Hanyu T (2003) Geochemical modeling of dehydration and partial melting of subducting lithosphere: toward a comprehensive understanding of high-Mg andesite formation in the Setouchi volcanic belt, SW Japan. Geochem Geophys Geosyst 4, Article Number: 1081

Tatsumi Y, Stern RJ (2006) Manufacturing continental crust in the subduction factory. Oceanography 19:104–112

Tatsumi Y, Shukuno H, Tani K, Takahashi N, Kodaira S, Kogiso T (2008) Structure and growth of the Izu-Bonin-Mariana arc crust: 2. Role of crust-mantle transformation and the transparent Moho in arc crust evolution. J Geophys Res 113, Article Number: B02203

Taylor B, Martinez F (2003) Back-arc basin basalt systematic. Earth Planet Sci Lett 210:481–497

Toth J, Gurnis M (1998) Dynamics of subduction initiation at pre-existing fault zones. J Geophys Res 103:18053–18067

Tsuchiya N, Suzuki S, Kimura J-I, Kagami H (2005) Evidence for slabmelt/mantle reaction: petrogenesis of Early Cretaceous and Eocene high-Mg andesites from the Kitakami Mountains, Japan. Lithos 79:179–206

Turner S, Foden J (2001) U, Th and Ra disequilibria, Sr, Nd, and Pb isotope and trace element variations in Sunda arc lavas: predominance of a subducted sediment component. Contrib Mineral Petrol 142:43–57

Turner S, Hawkesworth C (1997) Constraints on flux rates and mantle dynamics beneath island arcs from Tonga-Kermadec lava geochemistry. Nature 389:568–573

Turner S, Hawkesworth CJ, Rogers N, Bartlett J, Worthington T, Hergt J, Pearce JA, Smith IME (1997) 238U-230Th disequilibria, magma petrogenesis, and flux rates beneath the depleted Tonga-Kermadec island arc. Geochim Cosmochim Acta 61:4855–4884

Ueda K, Gerya T, Sobolev SV (2008) Subduction initiation by thermal–chemical plumes. Phys Earth Planet Inter 171:296–312

Uyeda S, Ben-Avraham Z (1972) Origin and development of the Philippine Sea. Nature 240:176–178

Van der Lee S, Regenauer-Lieb K, Yuen DA (2008) The role of water in connecting past and future episodes of subduction. Earth planet Sci Lett 273:15–27

Van Keken PE, King SD (2005) Thermal structure and dynamics of subduction zones: insights from observations and modeling. Phys Earth Planet Inter 149:1–6

van Keken PE, Kiefer B, Peacock SM (2002) High resolution models of subduction zones: implications for mineral dehydration reactions and the transport of water into the deep mantle. Geochem Geophys Geosyst 3, Article Number: 1056

Vlaar NJ, Wortel MJR (1976) Lithospheric aging, instability and subduction. Tectonophysics 32:331–351

Wyss M, Hasegawa A, Nakajima J (2001) Source and path of magma for volcanoes in the subduction zone of northeastern Japan. Geophys Res Lett 28:1819–1822

Yogodzinski GM, Volynets ON, Koloskov AV, Seliverstov NI, Matvenkov VV (1994) Magnesian andesites and the subduction component in a strongly calcalkaline series at the Piip volcano, far Western Aleutian. J Petrol 35:163–204

Yogodzinski GM, Lees JM, Churikova TG, Dorendorf F, Woerner G, Volynets ON (2001) Geochemical evidence for the melting of subducting oceanic lithosphere at plate edges. Nature 409:500–504

Zack T, Foley SF, Rivers T (2002) Equilibrium and disequilibrium trace element partitioning in hydrous eclogites (Trescolmen, central Alps). J Petrol 43:1947–1974

Zandt G, Gilbert H, Owens TJ, Ducea M, Saleeby J, Jones CH (2004) Active foundering of a continental arc root beneath the southern Sierra Nevada in California. Nature (Lond) 431:41–46

Zhao DP (2001) Seismological structure of subduction zones and its implications for arc magmatism and dynamics. Phys Earth Planet Inter 127:197–214

Zhao DP, Hasegawa A, Horiuchi S (1992) Tomographic imaging of P and S wave velocity structure beneath north-eastern Japan. J Geophys Res 97:19909–19928

Zhao DP, Mishra OP, Sanda R (2002) Influence of fluids and magma on earthquakes: seismological evidence. Phys Earth Planet Inter 132:249–267

Zhu G, Gerya TV, Yuen DA, Honda S, Yoshida T, Connolly JAD (2009) 3-D Dynamics of hydrous thermalchemical plumes in oceanic subduction zones. Geochem Geophys Geosyst 10, Article Number Q11006

http://www.springer.com/978-3-540-88557-3

Arc-Continent Collision
Brown, D.; Ryan, P.D.
2011, XII, 988 p. 241 illus., 221 in color., Hardcover
ISBN: 978-3-540-88557-3